STUDY OF CONVERTER CONTROL STABILITY FOR TWO TERMINAL HVDC SYSTEMS

by

BHARTI PANDEY

Th
EE/1985/M
EE 1 1925
1985
M
PAN
STU

DEPARTMENT OF ELECTRICAL ENGINEERING
INDIAN INSTITUTE OF TECHNOLOGY, KANPUR
MARCH, 1985

STUDY OF CONVERTER CONTROL STABILITY FOR TWO TERMINAL HVDC SYSTEMS

A Thesis Submitted
In Partial Fulfilment of the Requirements
for the Degree of
MASTER OF TECHNOLOGY

by
BHARTI PANDEY

to the

DEPARTMENT OF ELECTRICAL ENGINEERING
INDIAN INSTITUTE OF TECHNOLOGY, KANPUR
MARCH, 1985

87566

EL-1985-M-PAN-SIU

DEDICATED TO

PUJYA GURUJI

PT. WASUDEV RAMESHWAR TIWARI

14/3/85

CERTIFICATE

It is to certify that this work entitled 'STUDY OF CONVERTER CONTROL STABILITY FOR TWO TERMINAL HVDC SYSTEMS' by Bharti Pandey has been carried out under my supervision and that this work has not been submitted elsewhere for the award of a degree.

Sachchidanand

Dr. Sachchidanand
Department of Electrical Engineering
Indian Institute of Technology
Kanpur, India

POST
This
Kanpur
10/3/85

ACKNOWLEDGEMENT

With profound sense of gratitude, I take this opportunity to put on record my indebtedness and sincere thanks to my supervisor Dr. Sachchidanand for his insightful guidance and constant encouragement. He has been extremely patient in discussing each and every problem and [illegible] rendered his unreserved help throughout the work.

I am grateful to Dr. L.P. Singh for his inspiration and sincere advice.

My sincrest thanks are due to all my friends who took all possible care and pains in the completion of this work. In this connection I would like to make a special mention of Nirmal, Saurav, Senthil, Ajay, Ajit, Deepayan, Sahidul, Debojyoti, Madhumita and Jayshree.

Last, but not the least, I am thankful to Shri Bajpai for excellent drafting and Shri Yogendra for his efficient typing. Thanks are due to Shri Triveni Tiwari and Shri Gangaram for quick cyclostyling.

BHARTI PANDEY

LIST OF CONTENTS

Page

LIST OF FIGURES vii

LIST OF TABLES viii

ABSTRACT ix

CHAPTER 1 INTRODUCTION

1.1 General 1

1.2 Stability Analysis of Converter Control System 2

1.3 Objective and Scope of the thesis 6

1.4 Chapterwise Description of the thesis 7

CHAPTER 2 DEVELOPMENT OF HVDC SYSTEM MODEL

2.1 Introduction 9

2.2 Converter Representation 10

2.3 DC Transmission Line 14

2.4 Converter Controller 17

2.4.1 Current Controller 17

2.4.2 Power Controller 19

2.4.3 Predictive Type Extinction Angle Controller 19

2.4.4 Feedback Extinction Angle Controller 20

2.5 Firing Scheme 21

2.6 Single Converter Stability Analysis 25

2.7 Result and Discussion 29

2.8 Conclusion 31

Page

CHAPTER 3 STABILITY INVESTIGATION OF TWO TERMINAL HVDC SYSTEMS

3.1 Two Terminal HVDC System Model 32
3.2 Effect of Firing Control Scheme 36
3.3 Effect of Control Structure 46
3.4 Effect of Power Control at Rectifier 47
3.5 System Stability with Inverter under Constant-β Control 49
3.6 Effect of Variation in System Parameters 53
3.7 Conclusion 59

CHAPTER 4 TWO TERMINAL HVDC SYSTEM STABILITY WITH DIODE BRIDGE RECTIFIER

4.1 Model Formulation 60
4.2 Results 63
4.3 Conclusion 63

CHAPTER 5 CONCLUSION

5.1 Operating point Stability 66
5.2 Scope for Future Work 68

APPENDIX A OPERATING CONDITIONS AND SYSTEM PARAMETERS

A-1 Single Converter System 70
A-2 Two Terminal HVDC System 70
A-3 Two Terminal HVDC System with Diode Bridge Rectifier 73

Page

APPENDIX B DISCRETIZATION OF CONTINUOUS TIME STATE EQUATION 74

APPENDIX C MODEL FORMULATIONS

C-1 Controller Model for Case 6 of Table 3.1 76

C-2 Constant β Converter-Controller at Inverter 79

REFERENCES 81

LIST OF FIGURES

Fig. No.	CAPTION	Page
2.1	3 Valve Conduction of Converter	11
2.2	DC Transmission Line	15
2.3(a)	Block Diagram of Current Controller	18
2.3(b)	Block Diagram of Power Controller	18
2.3(c)	Block Diagram of CEA Controller	18
2.4	Equidistant Pulse Controller	24
2.5	Block Diagram of Single Converter	26
2.6	Stability Domain for Single Converter System	30
3.1	Frequency Response for Case 1 of Table 3.1	39
3.2	Frequency Response for Case 2 of Table 3.1	40
3.3	Frequency Response for Case 4 of Table 3.1	41
3.4	Frequency Response for Case 6 of Table 3.2	42
3.4(a)	Frequency Response for case 4 of Table 3.2	43
3.5	Effect of Firing Scheme	45
3.6	Effect of Control Structure	48
3.7	Effect of Power Controller	51
3.8	Stability Boundaries for Constant β Control	52
3.9	Effect of Source Inductance	54
3.10	Effect of Transmission Line Length	57
3.11	Effect of Extinction Angle	58
4.1	Stability Boundaries for Diode Bridge at Rectifier	64
C.1	Controller at Rectifier for Constant Current	77
C.2	Controller at Inverter for Constant γ	77
C.3	Controller at Inverter for Constant β	77

LIST OF TABLES

		Page
TABLE 3.1	Cases for Effect of Firing Scheme	37
TABLE 3.2	Cases for Effect of Control Structure	37
TABLE 3.3	Cases for Effect of Power Controller	50
TABLE 3.4	Cases for Effect of Source Inductance	50
TABLE 3.5	Cases for Effect of Transmission Line Length.	56

ABSTRACT

This thesis reports on the detailled investigation of the stability characteristics of two terminal HVDC system for the purpose of controller design with current and power control at rectifier terminal and feedback type of constant extinction angle control at the inverter. Both individual phase and equidistant pulse control firing schemes are considered. The effect of the variation in the control system structure, control strategies and system parameters is investigated. The operating point stability analysis, to accomplish this, is carried out using a linearized, discrete time state space system model based on average system quantities. The stability analysis is carried out using linear control theory techniques in both frequency and time domain.

CHAPTER 1

INTRODUCTION

1.1 GENERAL

The introduction of HVDC links in the existing power systems has added a new dimension in bulk power transmission over long distances. Apart from overcoming certain disadvantages of ac power transmission, the HVDC transmission has played an important role in improving the stability of the present day ac power system. The proper and reliable operation of HVDC system largly depends on the design of the associated control system. With multiterminal HVDC systems being envisaged in near future, the requirement for the proper design of converter controllers has assumed great importance as multiterminal operation requires a well coordinated control.

One of the primary requirements of the converter control system is to ensure reliable system performance in the event of certain disturbances normally encountered in operation. This demands a systematic approach for the design of the converter control systems.

The design of the converter controllers has been carried out using HVDC simulators or digital simulation.

Both these methods are quite costly and have restricted flexibility. This has necessitated the development of analytical methods to investigate the system stability for the design of converter control system. The analytical approach is more flexible and affords ease in studying various control alternatives with wide variation in controller parameters.

1.2 STABILITY ANALYSIS OF CONVERTER CONTROL SYSTEM

The HVDC system consists of converters, controllers, firing pulse generators, DC transmission network and the associated AC system. The study of system performance requires the dynamic representation of these components. The degree of details to be included in the representation depends on the type and objective of the study. For example, in case of transient stability studies [20] a simplified model of the converter is adequate. However, the operating point stability analysis (dynamic stability analysis) for the purpose of the design of converter controls, requires a detailed representation of the converter characteristics - alongwith the detailed dynamic representation of the associated control, firing pulse generation scheme, transmission network and the ac system. The dynamic interaction between these various components leads to a nonlinear mathematical model of the HVDC system.

The operating point stability analysis is however, carried out by linearising the set of equations around an operating point which then results in the linearised system model. The system stability can then be investigated using frequency response technique or eigen value analysis as applicable to the linear control system study.

Several HVDC system models have been reported in the literature for the purpose of operating point stability analysis. Basic difference between these models is due to the converter representation. Since the control of the converter is effective only at discrete time instants which correspond to the instants of firing, the converter and the associated firing pulse generator have been represented as discrete time systems. [1,2] . This leads to a discrete time description of the HVDC system. However, the converter has also been modelled as a continuous time system, thus resulting in a continuous time representation of the overall system.[19]

Acknowledging the discrete nature of converter control, Busemann [15] in 1951, first gave a system model in which the converter was represented by a constant dc gain for all frequencies. The effects of commutation and the dc side ripples were neglected. It was also pointed out that the phenomenon of hunting in rectifiers took place at half the firing frequency.

An interesting method has been suggested by Persson (6) for calculating the transfer function of a converter in a grid controlled system. A'conversion factor' is introduced which relates the instantaneous ac quantity with the corresponding dc quantity. Conversion factor, is defined as a periodic time function with its fundamental frequency equal to the supply frequency. Sakuma and Pacific interties are analysed to prove its practicability.

Fallside et. al.[4] developed the concept of modelling a converter as a pure sampler. To avoid the undesirable feature of harmonic instability, the effect of ripples fed back in a closed loop control system has been considered. Describing function technique has been employed for the design of the control system.

A new discrete time converter model was introduced by Sucena-Paiva et al [11] to include the effect of commutation. The changes in the converter output voltage were treated as impulses at the firing instant and at the end of the commutation period. As a result of this the converter was represented, for the purpose of small signal analysis, as a sampler. The stability analysis is carried out based on sampled data control theory using Z transform technique. The model has later been applied to investigate the system stability with VCO based firing control scheme [13] . The stability analysis of the HVDC systems connecting strong and weak ac systems have also been reported employing the discrete converter model [14,12] . However, the use of Z transfrom technique for stability analysis makes the development of the system model extremely cumbersome, particularly when the dynamic interaction between the ac and dc systems is included. [12]

Padiyar et al [1] have proposed a discrete time converter model based on average system quantities. Utilizing this, the overall HVDC system model is developed in the state space frame-work. The modular approach for the development of the system model enables to include the component representations to any desired degree of detail. The interaction between the ac and dc system dynamics has been represented by modelling the ac system in d-q frame of reference. The results of stability predictions are validated using digital simulation.

The stability analysis of HVDC system involving digital control has been carried out by Zhou [16]. A 'state-averaging' technique has been used to represent the discrete time instants of converter control in the development of the state space model of the HVDC system.

1.3 OBJECTIVE AND SCOPE OF THE THESIS

A review of the literature reveals that although various approaches have been put forward for the representation of the HVDC system, a detailed investigation of the stability characteristic of the HVDC system has not been carried out to study the effectiveness of the converter control system with different firing control schemes and change in system parameters.

The objectives of this thesis, therefore, are the following

1. Development of the two terminal HVDC system model considering a feedback type of control at the inverter.
2. Study of the effect of both individual phase control and equidistant pulse control firing schemes, on the stability characteristics of the system.
3. Detailed investigation of the system performance with different control strategies, variation in system parameters.

In this thesis the operating point stability analysis of the converter control system has been carried out for the purpose of controller design. The model of two terminal HVDC system is developed based on the approach outlined in reference [1] . The ac system feeding the converter is assumed to be strong and hence its dynamics representation is ignored.

1.4 CHAPTERWISE DESCRIPTION OF THE THESIS

Study of stability performance of two terminal HVDC system is carried out on the basis of a discrete linear model. Chapter 2 of the thesis deals with the development of **component models** of the system. Converter, controller, firing pulse generator and DC transmission line are modelled **individually in detail to** facilitate an overall model development. A typical case of single converter has also been taken up in this chapter to show the effect of firing schemes on the stability of the system.

Utilising the subsystem models developed in Chapter 2, a discrete-time linear model has been developed in Chapter 3 for carrying out the stability analysis. An attempt has been made to describe the interfacing of different subsystems in a systematic manner. The influence of firing schemes, different control structures, control strategies and system parameters have also been investigated in this chapter.

Chapter 4 is devoted to the development of a two terminal HVDC system model consisting of a diode bridge rectifier. The stability boundary for this case is deduced and compared with cases having thyristor-bridges at both the converters.

Chapter 5 reviews the major contribution of the thesis and suggests the future scope of the work.

CHAPTER 2

DEVELOPMENT OF HVDC SYSTEM MODEL

2.1 INTRODUCTION

The development of the HVDC system model for the purpose of dynamic stability analysis involves adequate representation of the dynamic characteristics of the various subsystems constituting the HVDC system. The subsystems involved are converters, controllers, firing pulse generators and d.c. transmission line. Of these subsystems, the converters and the firing pulse generators are the discrete time systems, while the controllers and the dc transmission network can be treated as continuous time systems. Because of the involvement of both continuous and discrete time subsystems, the development of the overall system model becomes quite complex. Therefore, in order to simplify the analysis, the following assumptions are made.

1. The time interval between two consecutive firing instants is constant and is equal to 60° for a 6 pulse converter.
2. The ac and dc side harmonics are neglected. This enables to neglect the filter representation on both ac and dc sides and permits the use of average values of the dc quantities and fundamental components of the ac quantities without leading to significant errors [12].

The development of the various subsystem models is described in this chapter based on these assumptions. However, due to the inherent nonlinear characteristics of the converter, the analysis is undertaken using linearized subsystem models. The controller and the transmission line are represented by the continuous time dynamic equations in the state space framework. The equations are then discretized and combined with the discrete time representation of the converter and the firing pulse generator to result in the linearized, state-space model of the two terminal HVDC system.

The converter representation alongwith the approach for the model formulation is illustrated in this chapter through the stability analysis of a single converter system feeding a load. A detailed stability investigation of a two terminal HVDC system is, however, taken up in the next chapter.

2.2 CONVERTER REPRESENTATION

The approach employed for the representation is the same as introduced in reference [2]. A balanced 3 phase, 6 pulse, bridge converter under 3 valve conduction is shown in Figure 2.1.

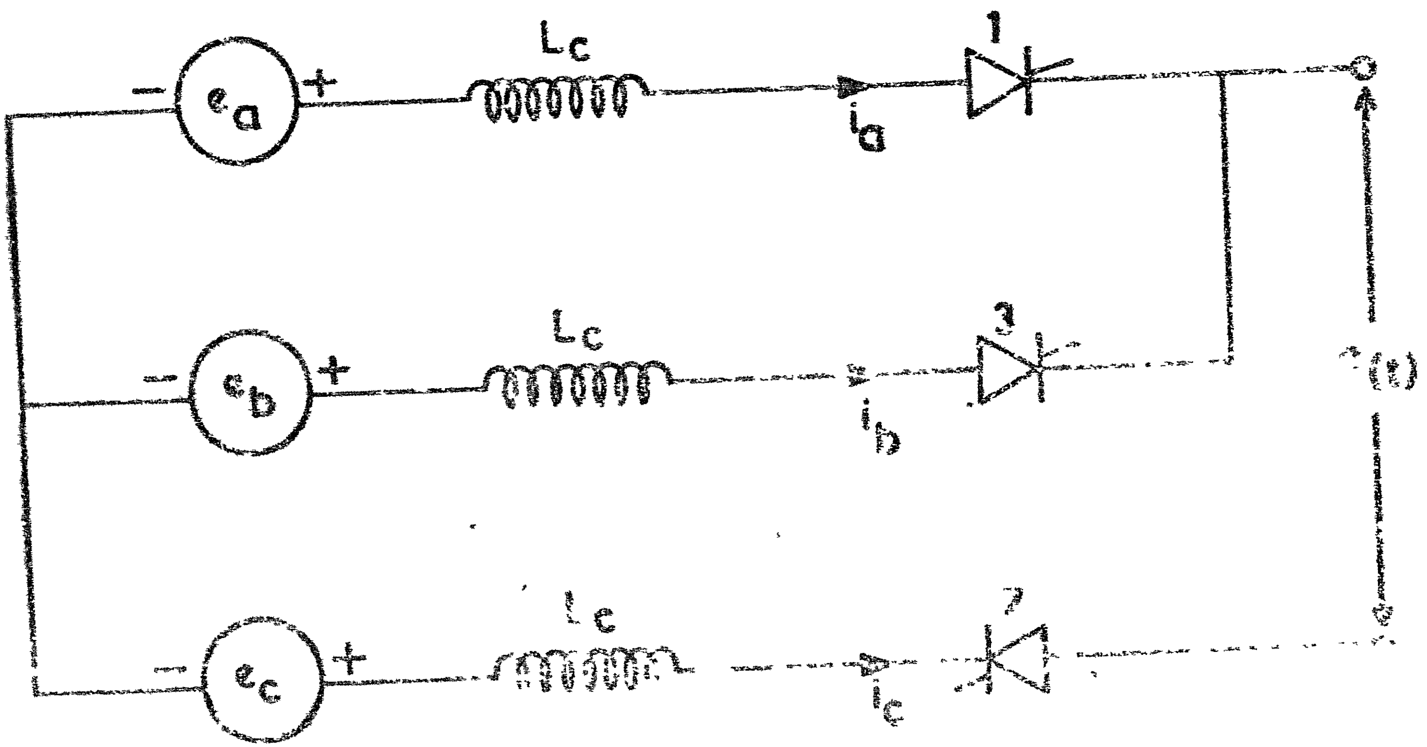

FIG. 2.1 3 VALVE CONDUCTION OF CONVERTER.

(Graetz Bridge)

The three phase ac voltages are given as

$$e_a = \sqrt{2}\; E_{ph} \operatorname{Sin} (w_o t + \frac{5\pi}{6})$$

$$e_b = \sqrt{2}\; E_{ph} \operatorname{Sin} (w_o t + \frac{\pi}{6}) \qquad \text{-- (2.1)}$$

$$e_c = \sqrt{2}\; E_{ph} \operatorname{Sin} (w_o t - \frac{\pi}{2})$$

Where E_{ph} is the rms ac phase voltage. Considering the converter transformer leakage inductance as L_c and neglecting the transformer resistance, an equation for the circuit shown in Figure 2.1 is written as

$$e(t) = e_b - e_c - L_c \frac{di_b}{dt} - L_c \frac{di_c}{dt} \qquad \text{-- (2.2)}$$

It is assumed that valve 3 starts conduction after a delay angle $\alpha(K)$, corresponding to the time instant $t(K)$. The delay angle is measured with respect to positive going zero crossing of the commutation voltage. The next valve starts conduction at the instant $t(K+1)$. The average dc output voltage of the converter over the interval of time $t(K)$ to $t(K+1)$ is given by

$$V_{dc}(K) = \frac{1}{\Delta t(K)} \int_{t(K)}^{t(K+1)} e(t)\, dt \qquad \text{-- (2.3)}$$

As per assumption, valves begin conduction at a regular interval of 60°. Which implies that

$$\Delta t(K) = \frac{\pi}{3w_o} \qquad \text{-- (2.4)}$$

w_o is the angular frequency corresponding to the ac system frequency.

Equation (2.3) with the help of equation (2.2) is rewritten as

$$V_{dc}(K) = \frac{1}{\Delta t_K} \int_{\alpha_{(K)}/w_o}^{(\alpha_{(K)}+\frac{\pi}{3})/w_o} (e_b - e_c - L_c\frac{di_b}{dt} - L_c\frac{di_c}{dt})\,dt \qquad \text{-- (2.5)}$$

At the instant $t(K)$ Valve 3 starts conduction making i_b equal to zero and i_c equal to converter dc current $I_{dc}(K)$. At the next instant $t(K+1)$, i_b equals $I_{dc}(K+1)$, which is the same as i_c. The equation, (2.5) therefore, is reduced to

$$U_{DC}(K) = \frac{\sqrt{2}E}{w_o}\cos\alpha(K) - 2\,L_c\,I_{dc}(K+1) + L_c\,I_{dc}(K) \qquad \text{-- (2.6)}$$

WHERE E = LINE TO LINE RMS VOLTAGE

Such that

$$V_{dc}(K) \triangleq \frac{U_{DC}(K)}{\Delta t_K} \qquad \text{-- (2.7)}$$

The converter model can be modified for small perturbation by linearising equations (2.6) and (2.7), at the operating point, as

$$\Delta V_{dc}(K) = \frac{\Delta U_{DC}(K)}{\Delta t_k} \qquad \text{-- (2.8)}$$

where $\Delta U_{DC}(K) = A_1 \Delta \alpha(K) + A_2 \Delta I_{dc}(K+1) + A_3 \Delta I_{dc}(K)$

$$\text{-- (2.9)}$$

in which $A_1 = -\frac{\sqrt{2E}}{w_o} \text{Sin } \alpha_o$; $A_2 = -2L_c$; $A_3 = L_c$

α_o is the firing angle at operating point. E is assumed to be constant as the ac system is considered to be strong.

2.3 D.C. TRANSMISSION LINE

An equivalent 'T' network of dc transmission line having lumped parameters is shown in Figure 2.2. Linear differential equations describing the transmission line dynamics are derived with converters represented as equivalent dc voltage sources at the rectifier and inverter ends. Between the dc voltage source and the transmission line, smoothing reactors to limit the overcurrents are also considered.

A state space equation for the transmission line is given by

$$\Delta \dot{\underline{X}}_N = [A_N] \Delta \underline{X}_N + [B_N] \Delta \underline{V}_{dc}(K) \qquad \text{-- (2.10)}$$

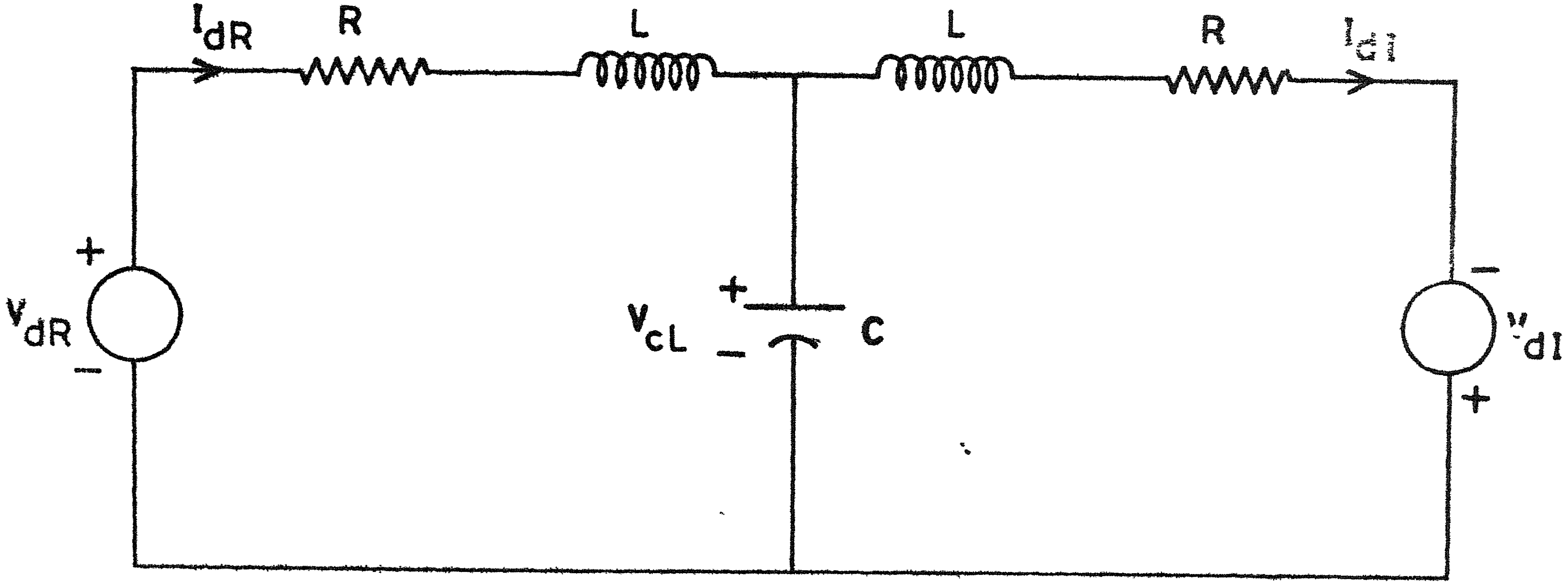

FIG. 2.2 DC TRANSMISSION LINE.

where $[A_N] = \begin{bmatrix} -R/L & 0 & -1/L \\ 0 & -R/L & 1/L \\ 1/C & -1/C & 0 \end{bmatrix}$ and $[B_N] = \begin{bmatrix} 1/L & 0 \\ 0 & 1/L \\ 0 & 0 \end{bmatrix}$

$$\Delta \underline{X}_N^T = [\Delta I_{dR} \quad \Delta I_{dI} \quad \Delta V_{cL}]$$

R is the sum of smoothing reactor resistance and half of the transmission line resistance. Similarly L is also the sum of the smoothing reactor inductance and half of the transmission line inductance. V_{CL} is the voltage across transmission line capacitance. I_{dR} and I_{dI} are the dc currents at the rectifier and inverter ends respectively. Output equation of the transmission line is

$$\Delta \underline{Y}_N = [C_N] \; \Delta \underline{X}_N \qquad \text{-- (2.11)}$$

where the constant matrix $[C_N] = \begin{bmatrix} 1 & 0 & 0 \\ 0 & 1 & 0 \end{bmatrix}$

$\Delta \underline{Y}_N$ represents the vector of converter dc currents.

2.4 CONVERTER-CONTROLLERS

The converter is generally equipped with constant power or constant current controller when operating as a rectifier, and constant extinction angle when operating as an inverter. While current and power controllers are of feed-back type, the constant extinction angle controller as discussed in the literature [7, 8] can be either of predictive type or of feed-back type. In what follows, the dynamic equations of the various controllers are developed.

2.4.1 Current Controller

The converter output dc current is fed back in the controller loop. This is compared with reference current. The error, thus obtained, is then amplified through controller amplifier to give control signal which is further sent to the firing pulse generator. Figure 2.3(a) shows the block diagram of current controller.

The state and output equations depending upon the transfer function of controller amplifier is written as

$$\Delta \dot{\underline{x}}_{CC} = [A_{CC}] \quad \Delta \underline{x}_{CC} + \underline{B}_{CC} \Delta u_{CC} \qquad \text{-- (2.12)}$$

and $$\Delta y_{CC} = \underline{C}^{T}_{CC} \quad \Delta \underline{x}_{CC} \qquad \text{-- (2.13)}$$

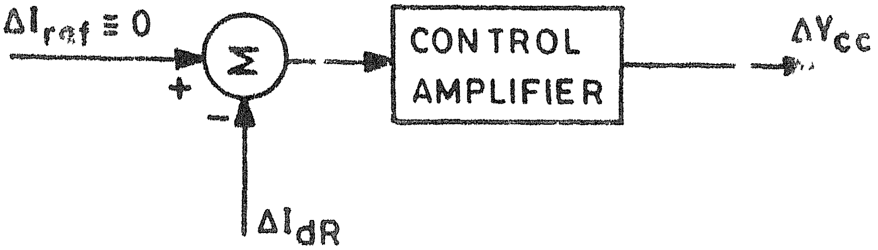

FIG. 2.3(a) BLOCK DIAGRAM OF CURRENT CONTROLLER.

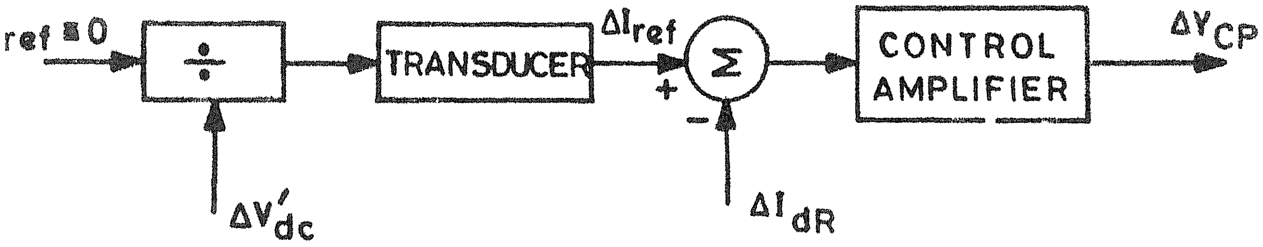

where V'_{dc} is the average of rectifier and inverter voltage'

FIG. 2.3(b) BLOCK DIAGRAM OF POWER CONTROLLER

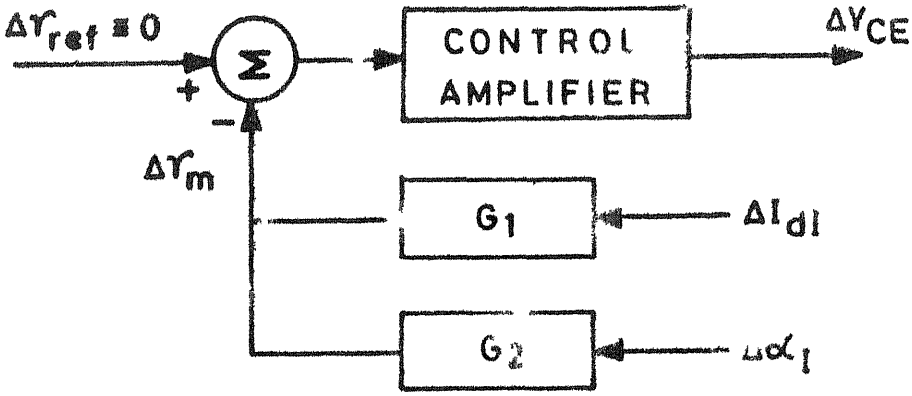

FIG. 2.3(c) BLOCK DIAGRAM OF C E A CONTROLLER

where $\underline{X}_{CC}$ is the state vector, Y_{CC} is the control signal output and ΔU_{CC} is the converter dc current (feedback signal) obtained as output of transmission line model. The variation in the current reference setting is neglected assuming the steady state of system operation.

2.4.2 Power Controller

The block diagram of a power controller is shown in Figure 2.3(b). The current reference is determined from a power reference. The following is the state and output equations representing a power controller.

$$\Delta \dot{\underline{X}}_{PC} = [A_{PC}]\, \Delta \underline{X}_{PC} + \underline{B}_{PC} \quad \Delta U_{PC} \qquad \text{-- (2.14)}$$

$$\Delta Y_{PC} = \underline{C}^{T}_{PC} \quad \Delta \ \underline{X}_{PC} \qquad \text{-- (2.15)}$$

where Y_{PC} is the controller output.

2.4.3 Predictive Type Constant Extinction Angle (C.E.A.) Controller

The available information of ac voltage and direct ~~cu~~ current is utilized to predict the value of extinction angle [9]. Discrete time equation of the CEA control is

$$- \sqrt{2}E \cos \alpha(K) - \sqrt{2}E \cos \gamma_c + 2\, w_o L_c\, I_{dc}(K) = 0 \qquad \text{-- (2.16)}$$

where α, γ_c are the firing and extinction angles respectively.

Under the assumption of constant ac system voltage, the equation (2.15) upon linearization gives

$$\Delta \alpha(K) = - \frac{\sqrt{2} w_o L_c}{E \sin \alpha_o} \Delta I_{dc}(K) \qquad (2.17)$$

2.4.4 Feedback Extinction Angle Controller

Predictive type CEA control is an open loop control. To make the system insensitive to external disturbances a more accurate method is to use a closed loop control for extinction angle. A block diagram is given in Figure 2.3(c), which shows the arrangement of a feedback (closed loop) extinction angle controller.

Feedback signal is the variation in the measured value of extinction angle which is obtained using the following equation [3] .

$$I_d = \frac{\sqrt{2}E}{2wL_c} (\cos \alpha + \cos \gamma_m) \qquad -- (2.18)$$

where E is the rms line voltage at inverter end, L_c is the leakage inductance of the converter transformer and γ_m is the measured value of extinction angle.

Equation (2.18) upon linearization yields

$$\Delta \gamma_m = G_1 \Delta I_d + G_2 \Delta \alpha_{(K)} \qquad -- (2.19)$$

where $G_1 = \frac{-\sqrt{2}\, wL_c}{E \sin \gamma_o}$ and $G_2 = \frac{-\sin \alpha_o}{\sin \gamma_o}$

$\alpha_{(K)}$ is the inverter delay angle at the K^{th} instant, obtained as the output of the firing pulse generator to which the input is the control signal output.

The controller dynamics can be obtained in a general form as

$$\Delta \dot{\underline{X}}_E = [\, A_E \,] \; \Delta \underline{X}_E + \underline{B}_E \; \Delta U_E \qquad \text{-- (2.20)}$$

$$\Delta Y_E = \underline{C}_E^T \; \Delta \underline{X}_E \qquad \text{-- (2.21)}$$

ΔY_E is the control signal output. The input ΔU_E comprises of the inverter end dc current and firing angle at K^{th} instant.

2.5 FIRING SCHEME

A satisfactory operation of the converter can be assured only when the firing pulses are accurately timed. HVDC links particularly use two types of firing control schemes - 1. Individual ~~Pulse~~ Phase Control (I.P.C.) and 2. Equidistant Pulse Control (E.P.C.).

In individual ~~pulse~~ phase control firing scheme each valve is controlled independently and the firing instants are determined in each cycle based on the commutation voltage of the particular valve. In IPC firing scheme considered here a ramp is generated at each positive going zero crossing of the commutation voltage and is compared with the control signal output obtained from the controller. At the instant of equality, the firing pulse is generated. [11]

For a small change in control signal ΔV_C, the corresponding change in the firing angle is related as

$$\Delta \alpha(K) = K_{fs} \Delta V_C(K) \qquad \text{-- (2.22)}$$

where K_{fs} is the slope of ramp, which is the same as the gain of firing pulse generator.

It is evident that in IPC firing scheme, the generation of the firing instants critically depends on the commutation voltage waveform. In the case of HVDC system connected to weak ac systems, these commutation voltages are distorted due to the presence of harmonics. This gives rise to a problem of harmonic instability as reported in reference [9]. To circumvent this problem, equidistant pulse control firing scheme was first introduced by Ainsworth [[illegible]].

The block diagram structure of the EPC firing scheme based on pulse frequency control [10] is shown in Figure 2.4.

This scheme makes use of a voltage-controlled oscillator (VCO), the output of which controls a constant-slope ramp function generator. The sum of the voltage T/6, which is a constant bias for the VCO, and the control voltage are compared with the ramp signal. A pulse is generated at each instant of equality. Corresponding to steady state operation, the control voltage is zero and the consecutive firing pulses thus maintain a regular distance of 60°. The frequency of the oscillator is governed by the control signal. The dynamics of EPC firing pulse generator in its linearised form is given by

$$\Delta Z(K+1) = \Delta Z(K) + K_{fs} \cdot \Delta t_k \cdot \Delta V_C(K) \qquad \text{-- (2.23)}$$

Also,

$$\Delta \alpha(K) = \Delta Z(K) \qquad \text{-- (2.24)}$$

The subsystem models developed in the previous sections can be combined appropriately to yield the overall system model in the form [2] .

$$\Delta \underline{X}'(K+1) = [AA]\Delta\underline{X}'(K) + [BB]\ \Delta \underline{U}_d(K) \qquad \text{-- (2.25)}$$

and $\Delta Y'(K) = \underline{CC}^T \quad \Delta \underline{X}'(K)$ -- (2.26)

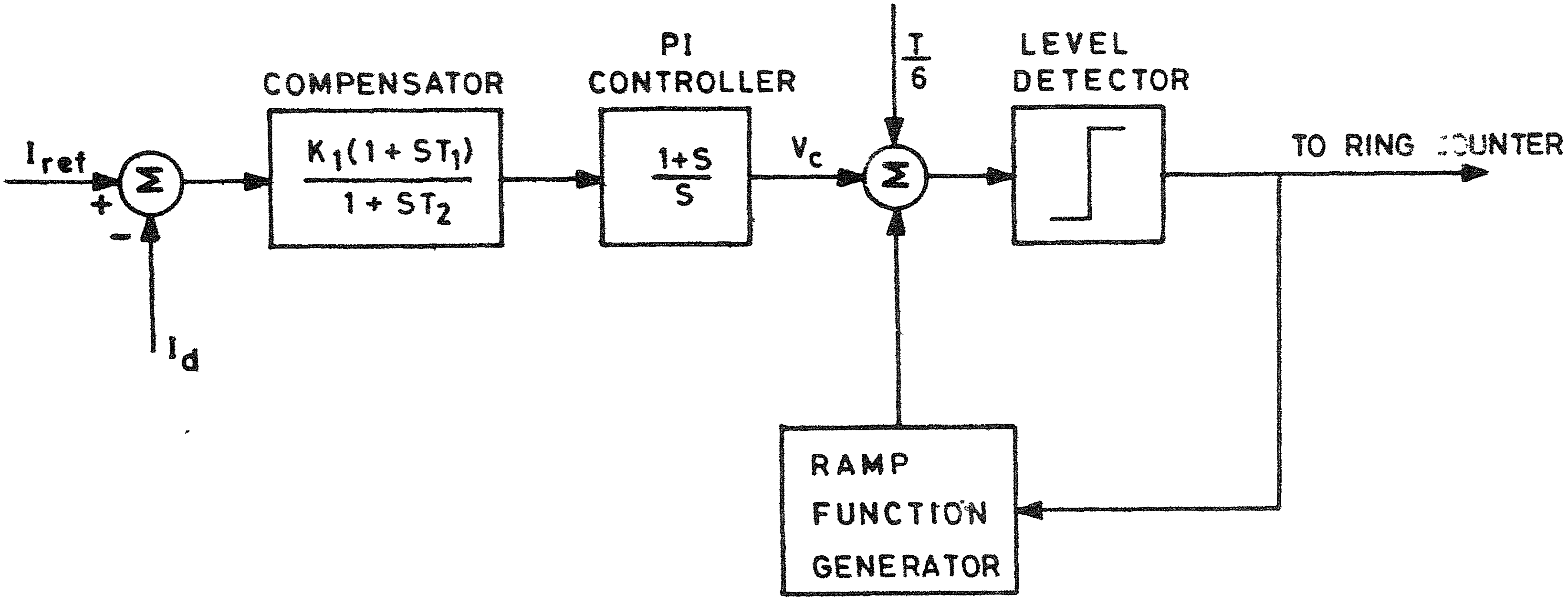

FIG. 2.4 EQUIDISTANT PULSE CONTROL.

The system stability can be investigated either from the eigen values of the closed loop system matrix or frequency response of the open loop transfer function $\Delta Y_{(s)} / \Delta U_{d(s)}$. The details of the approach to build the overall system model is given in the next chapter. However, in this chapter, the stability analysis of a single converter system is carried out to illustrate the converter representation and the approach for the development of the overall system model.

2.6 SINGLE CONVERTER STABILITY ANALYSIS

A single converter system feeding an R-L load is shown in Figure 2.5. The system stability is investigated under both IPC and EPC firing schemes. The system data and operating conditions are given in Appendix [A-1] . The gain of the firing control scheme is taken as unity.

Controller and load (continuous time subsystems) dynamics are described by the equation

$$\Delta \dot{\underline{X}} = [A] \Delta \underline{X} + \underline{B} \; \Delta V_{dc}(K) \qquad \text{-- (2.27)}$$

where

$$A = \begin{bmatrix} -\frac{1}{T_1} & K_1 \\ 0 & -\frac{1}{T_2} \end{bmatrix}; \qquad \underline{B} = \begin{bmatrix} 0 \\ 1/R\ T_L \end{bmatrix}$$

$$\Delta \underline{X}^T = [\Delta P \quad \Delta I_d].$$

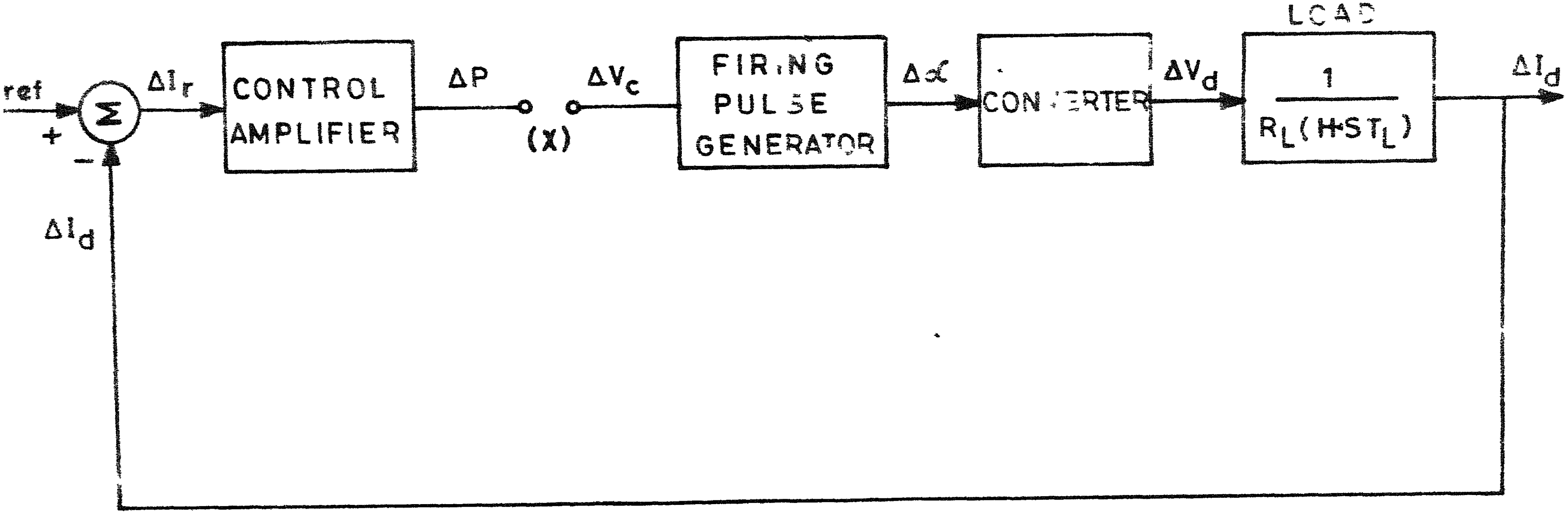

FIG. 2.5 BLOCK DIAGRAM OF SINGLE CONVERTER.

K_1 is the gain of control amplifier and T_1 is its time constant. R_L and T_L are the load resistance and time constant respectively.

In order to combine the continuous time equation (2.27) with the discrete equation for the converter and the firing pulse generator, equation (2.27) is discretized, using the technique discussed in Appendix [B], to give the following form.

$$\Delta \underline{X}(K+1) = e^{[A]H} \Delta \underline{X}(K) + [MD] \underline{B} \Delta V_{dc}(K) \quad \text{-- } (2.28)$$

converter equation (2.6) and equation (2.22) for IPC firing scheme are combined with equation (2.28) giving

$$\Delta \underline{X}(K+1) = [AA] \Delta \underline{X}(K) + \underline{BB} \Delta V_C(K) \quad (2.29)$$

In the case of EPC firing control scheme equation (2.28) is augmented to include the dynamics of the firing control scheme given by equation (2.23). The resulting equation is combined with equations (2.6) and (2.24) to yield.

$$\Delta \underline{X}'(K+1) = [A'] \Delta \underline{X}'(K) + \underline{B}' \Delta V_C(K) \quad \text{-- } (2.30)$$

where $\Delta \underline{X}'(K) = \begin{bmatrix} \Delta \underline{X}(K) \\ \Delta Z(K) \end{bmatrix}$; $[A'] = \begin{bmatrix} [AA] & 0 \\ 0 & 1 \end{bmatrix}$

and

$$\underline{B}' = \begin{bmatrix} \underline{BB} \\ 0 \end{bmatrix}$$

Equation (2.29) and (2.30), thus, represent the overall single converter system having an R-L load in a linear and discretized form with IPC and EPC firing schemes respectively.

Stability of the system is investigated using eigen value analysis and frequency response from open loop transfer function. The loop is opened at point (x) as shown in Figure 2.5 where the quantities are related as

$$\Delta V_C(K) = \Delta P_C(K) \qquad \text{.. (2.31)}$$

$\Delta P(K)$, in fact, is a component in the vector $\Delta X'(K)$. Therefore

$$\Delta V_C(K) = \underline{C}' \; \Delta \underline{X}'(K) \qquad (2.32)$$

Equation (2.31) is combined with equation (2.29) to give

$$\Delta \underline{X}'(K+1) = [\, A'' \,] \; \Delta \underline{X}'(K) \qquad \text{-- (2.33)}$$

$[A'']$ is a closed loop matrix, the eigen values of which would decide the stability of the system under consideration.

The frequency response is deduced after deriving an expression for the open loop transfer function. System equations (2.29) and (2.31) are transformed into frequency domain using classical Laplace transformation technique. The equations, hence can be written as

$$e^{S\Delta t_K} \quad \Delta \underline{X}'_{(s)} = [A']\Delta \underline{X}'_{(s)} + \underline{B}' \ \Delta V_{C(s)} \qquad \text{-- } (2.34)$$

and $$\Delta P_{(s)} = \underline{C}'_{(s)} \quad \Delta \underline{X}'_{(s)} \qquad \text{-- } (2.35)$$

Equations (2.34) and (2.35), therefore, decide the open loop transfer function as

$$\frac{\Delta P_{(s)}}{\Delta V_C(s)} = \underline{C}'_{(s)} \quad \left\{ [C''] - [A'] \right\}^{-1} \ \underline{B}' \qquad \text{-- } (2.36)$$

where $[C''] = e^{S\Delta t_K}[I]$; $[I]$ being a unity matrix.

2.7 RESULT AND DISCUSSION

Stability boundaries are plotted on the controller gain and time constant for both the IPC and EPC firing control schemes in Figure 2.6. The observation of the boundaries indicate that the EPC firing scheme is better than IPC within a range of time constants from 0.01 millisecond to 0.17 millisecond. At higher time constants it is seen that the stability domain is much larger with IPC firing control scheme as compared to that with EPC firing control. This trend conforms with results reported in references [2] and [8] .

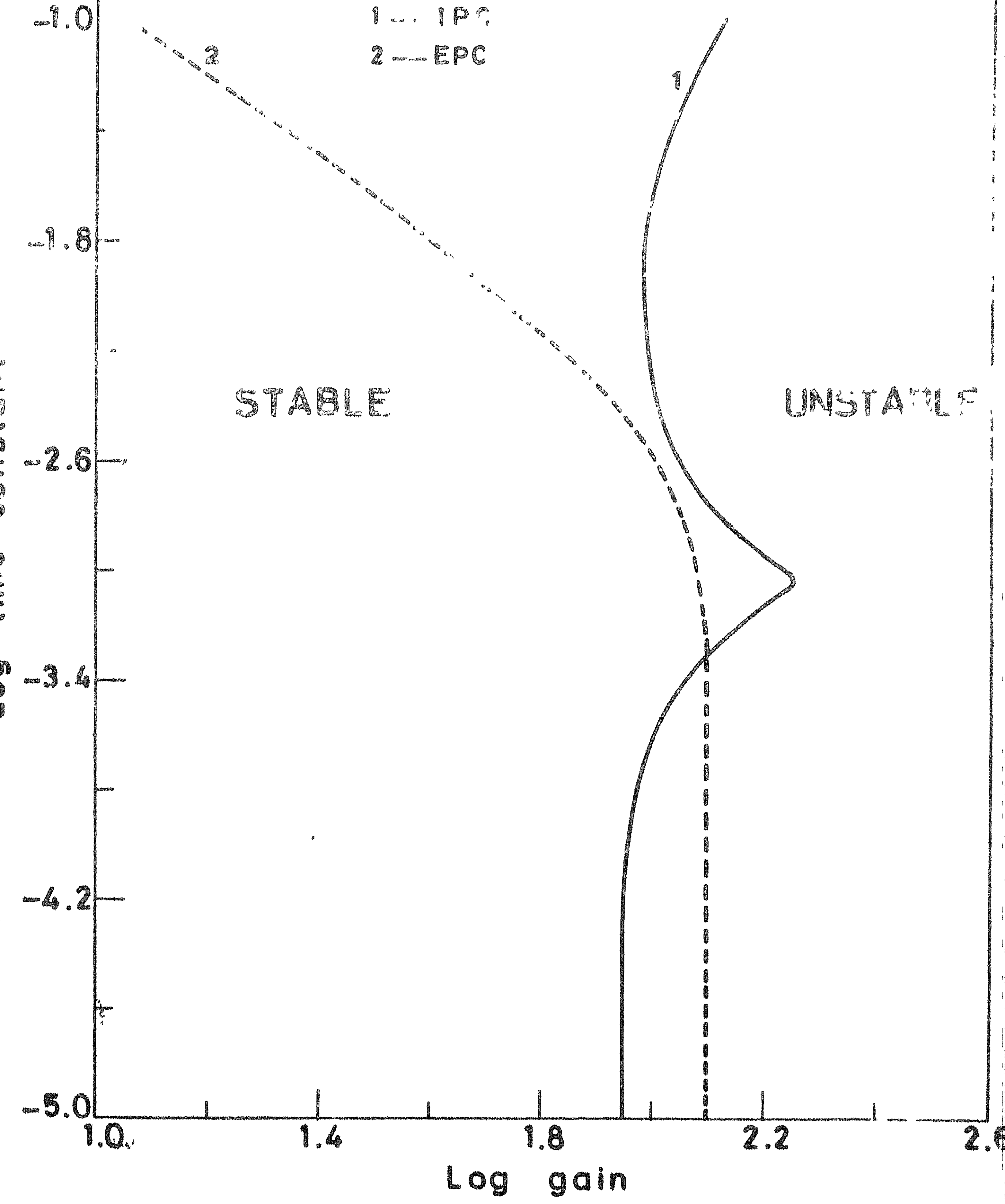

FIG. 2.6 STABILITY DOMAIN FOR SINGLE CONVERTER SYSTEM.

2.8 CONCLUSION

In this chapter, a detailed representation of various subsystems constituting an HVDC system is presented for the purpose of stability analysis. To illustrate the various component models, the stability study of a single converter system is carried out with both IPC and EPC firing schemes. The approach for the development of the overall system model is extremely modular as a result of which a subsystem can be represented to any degree of detail desired.

CHAPTER 3

STABILITY INVESTIGATION OF TWO TERMINAL HVDC SYSTEMS

A detailed stability analysis of converter control systems, considering the discrete nature of the control, for two terminal HVDC system has been carried out in this chapter. An overall model of the HVDC system is developed on the basis of subsystem models discussed in Chapter 2. The objective here is to investigate the system stability with different firing control schemes, controller structures and system parameters.

3.1 TWO TERMINAL HVDC SYSTEM MODEL

The component models for converter, controller, firing pulse generator and transmission line are developed in the previous chapter and utilized here to construct an overall model for the two terminal HVDC system.

The transmission line model remains unaltered which is given by equation (2.10) as

$$\Delta \dot{\underline{x}}_N = [A_N]\Delta \underline{x}_N + [B_N]\Delta \underline{v}_{dc}(K)$$

Depending upon the choice of controllers at both rectifier and inverter ends, their dynamics can be combined chosing appropriate equations from 2.12, 2.14, 2.20 to give the general form as

$$\Delta \dot{\underline{x}}_C = [A_C]\Delta \underline{x}_C + [B_C]\Delta \underline{u}_C(k) \qquad \text{-- (3.1)}$$

where $\underline{X}_C$ is the state vector containing variables associated with controller and $\underline{U}_C$ is the input vector which may be converter dc current, or delay angle $\alpha(K)$ depending upon the type of control system at the terminals.

Equations (2.10) and (3.1) can be written in the following manner to give the continuous time equation of the system as

$$\dot{\underline{X}} = [A]\,\Delta\underline{X} + [B]\,\Delta\underline{U}(K) \qquad \text{--- (3.2)}$$

where

$$[A] = \begin{bmatrix} [A_C] & [B_{CN}] \\ [0] & [A_N] \end{bmatrix} \quad ; \quad [B] = \begin{bmatrix} [B_C] \\ [B_N] \end{bmatrix}$$

$$\text{and } \Delta\underline{X} = \begin{bmatrix} \Delta\underline{X}_C \\ \Delta\underline{X}_N \end{bmatrix}$$

The interface between controller and the transmission network models is through the converter dc current which is obtained as the output of the transmission network model and goes as the input to the controller. This effect is incorporated in matrix $[A]$ through matrix $[B_{CN}]$.

Equation (3.2) is now discretized using the method given in Appendix [B] and is written in the form

$$\underline{X}(K+1) = [AA]\,\Delta\underline{X}(K) + [BB]\,\Delta\underline{U}(K) \qquad \text{-- (3.3)}$$

In case, EPC firing scheme is considered at any or both of the terminals, equation (3.4) is augmented to include the dynamics of the firing scheme given by

$$\Delta Z(K+1) = \Delta Z(k) + K_{fs}\,\Delta t_K\,\Delta V_C(K) \qquad \text{-- (3.4)}$$

$V_C(K)$ is the input to the firing pulse generator and is the same as the output of the corresponding controller. $\Delta\underline{U}(K)$ in equation (3.3) consists of $\Delta\underline{V}_{dc}(K)$ as its component. The latter can be obtained from the converter equations (2.6) and (2.7) as

$$\Delta\underline{V}_{dc}(K) = \frac{1}{\Delta t_K}\,\Delta\underline{U}_{DC}(K) \qquad \text{-- (3.5)}$$

where

$$\Delta\underline{U}_{DC}(K) = [P]\,\Delta\underline{\alpha}(K) + [Q]\,\Delta\underline{I}_d(K+1) + [R]\,\Delta\underline{I}_d(K) \qquad \text{-- (3.6)}$$

$$[P] = \begin{bmatrix} \dfrac{-2E_R \operatorname{Sin}\alpha_{R0}}{w_o} & 0 \\ 0 & \dfrac{-2E_I \operatorname{Sin}\alpha_{I0}}{w_o} \end{bmatrix}; \quad [Q] = \begin{bmatrix} -2L_{CR} & 0 \\ 0 & -2L_{CI} \end{bmatrix}$$

$$[R] = \begin{bmatrix} L_{CR} & 0 \\ 0 & L_{CI} \end{bmatrix}$$

$\underline{\alpha}_{(K)}$ in equation (3.6) is obtained from the equations (2.22) and (2.24); corresponding to the firing pulse generators associated with the rectifier and inverter terminals.

Combination of equation (3.4) with equations (3.5) and (3.6) after substituting for $\Delta\underline{\alpha}_{(K)}$ using the equations corresponding to the firing pulse generators, result in the following equation.

$$\Delta\underline{X}'(K+1) = [A']\,\Delta\underline{X}'(K) + \underline{B}'\,\Delta V_C(K) \qquad \text{-- (3.7)}$$

In case IPC firing scheme is considered, then discrete equation (3.3) is directly combined with equations (3.5) and (3.6) to give equation similar to the equation (3.7).

Since $\Delta V_C(K)$ in equation 3.7 is the output of the converter controller, it can be related to the state vector $\Delta\underline{X}$ and then the closed loop description of the overall system can be obtained in the form.

$$\Delta\underline{X}'(K+1) = [A'']\,\Delta\underline{X}'(K) \qquad \text{-- (3.8)}$$

Stability analysis can be carried out on the basis of eigen values of matrix $[A'']$. To investigate the system stability using the frequency response technique, the open loop transfer function is $\Delta P(S)/\Delta V_C(S)$ which can be obtained as shown in equation 2.36.

EXAMPLE : The stability analysis for a two terminal HVDC system is presented using the model developed earlier. Details about the system parameters and operating conditions are given in Appendix [A-2]. The effects of different firing schemes, controllers and system parameters are investigated.

3.2 EFFECT OF FIRING CONTROL SCHEME

The effects of IPC and EPC firing schemes have been discussed on a single converter model in the previous chapter. On the same lines a two terminal HVDC system is taken up to study the effect of firing control on stability performance.

The cases studied are listed in Table 3.1, alongwith the details of associated control structures and firing schemes used. The rectifier is considered to be under constant current control whereas the inverter is on constant extinction

TABLE 3.1

Cases for Effect of Firing Scheme

S. No.	Rectifier		Inverter	
	Control	Firing	Control	Firing
1	$\left[\frac{-K}{1+ST}\right]$	IPC	-	Predictive
2	"	EPC	-	Predictive
3	"	IPC	$\left[\frac{-K}{1+ST}\right]$	IPC
4	"	EPC	"	IPC
5	"	IPC	"	EPC
6	"	EPC	"	EPC

TABLE 3.2

Cases For Effect of Control Structure

S.No.	Rectifier		Inverter	
	Control	Firing	Control	Firing
1	$\left[\frac{-K}{1+ST}\right]$	IPC	-	Predictive
2	"	EPC	-	Predictive
3	$\left[\frac{-K(1+ST_1)}{1+ST_2}\right] . \left[\frac{1+S}{S}\right]$	IPC	-	Predictive
4	"	EPC	-	Predictive
5	"	IPC	$[-K] . \left[\frac{1+S}{S}\right]$	EPC
6	"	EPC	"	EPC

angle control. The details of the development of a model for case 6 of Table 3.1 are given in Appendix [C] .

The frequency response based on the open loop transfer function is obtained for the cases 1,2,4 and 6 of Table 3.1 and only the significant portion of it are plotted respectively in Figures 3.1, 3.2, 3.3 and 3.4. The converter-controller gain and time constants are indicated in Appendix [A-2]. The corresponding operating conditions and system parameters are also given in the same Appendix.

From Figures (3.1) and (3.2), it can be seen that the frequencies of oscillations at which instability is likely to occur are 16.9 Hz and 65.8 Hz with IPC and 1.3 Hz with EPC at rectifier when the inverter is at predictive type CEA controller. Introduction of IPC at inverter (Figure 3.3), does not alter the frequency of oscillation (1.3 Hz), but with use of EPC at inverter (case 6) it is slightly increased (7.3 Hz, refer Figure 3.4). Thus it is seen that the VCO based EPC firing scheme, which introduced an integral characteristic in the system, results in oscillations at lower frequencies. This effect of EPC has also been reported in reference [13] .

The stability characteristics of the system are further investigated through the stability boundaries obtained

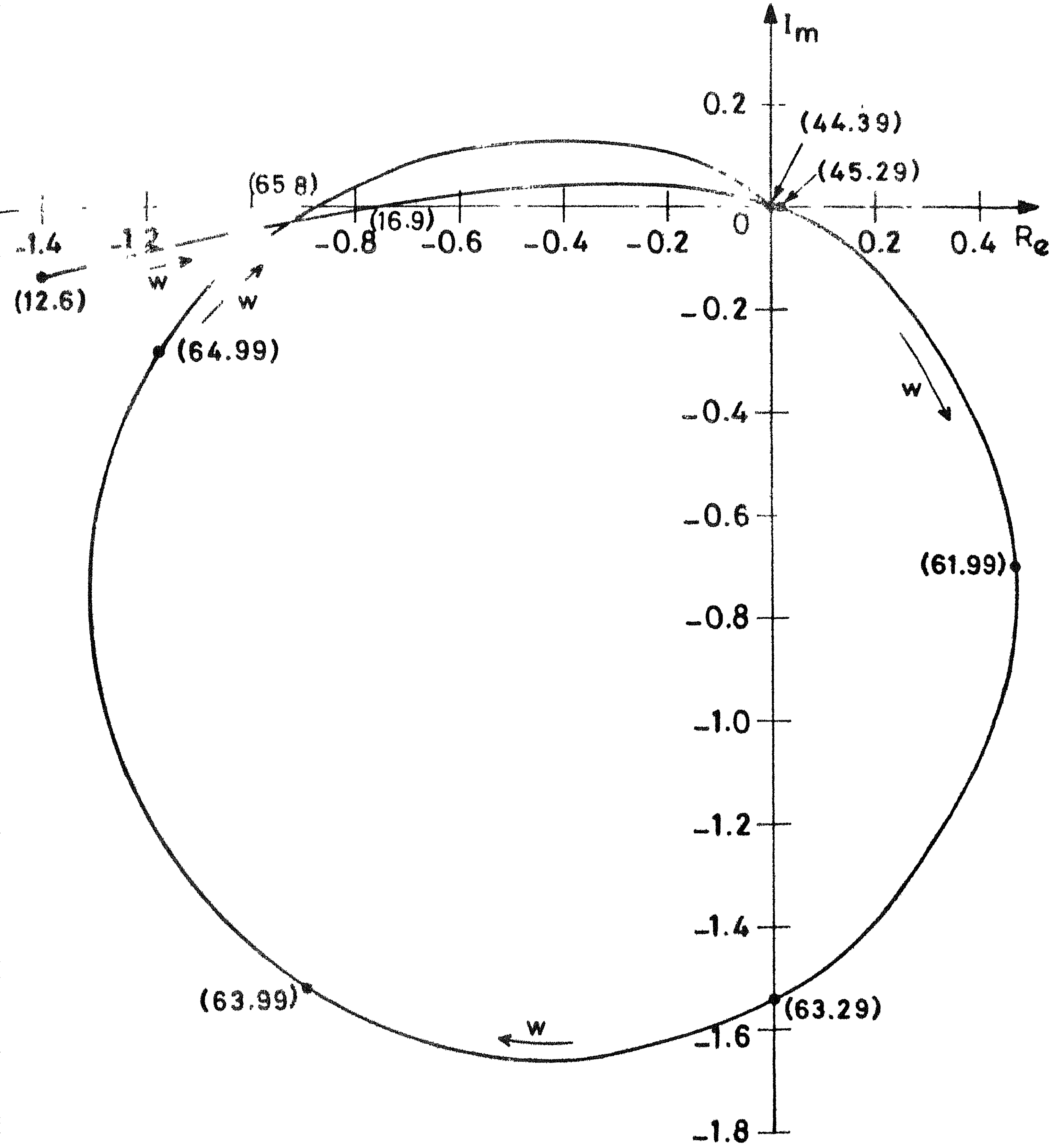

FIG. 3.1 FREQUENCY RESPONSE FOR CASE 1 OF TABLE [3.1]

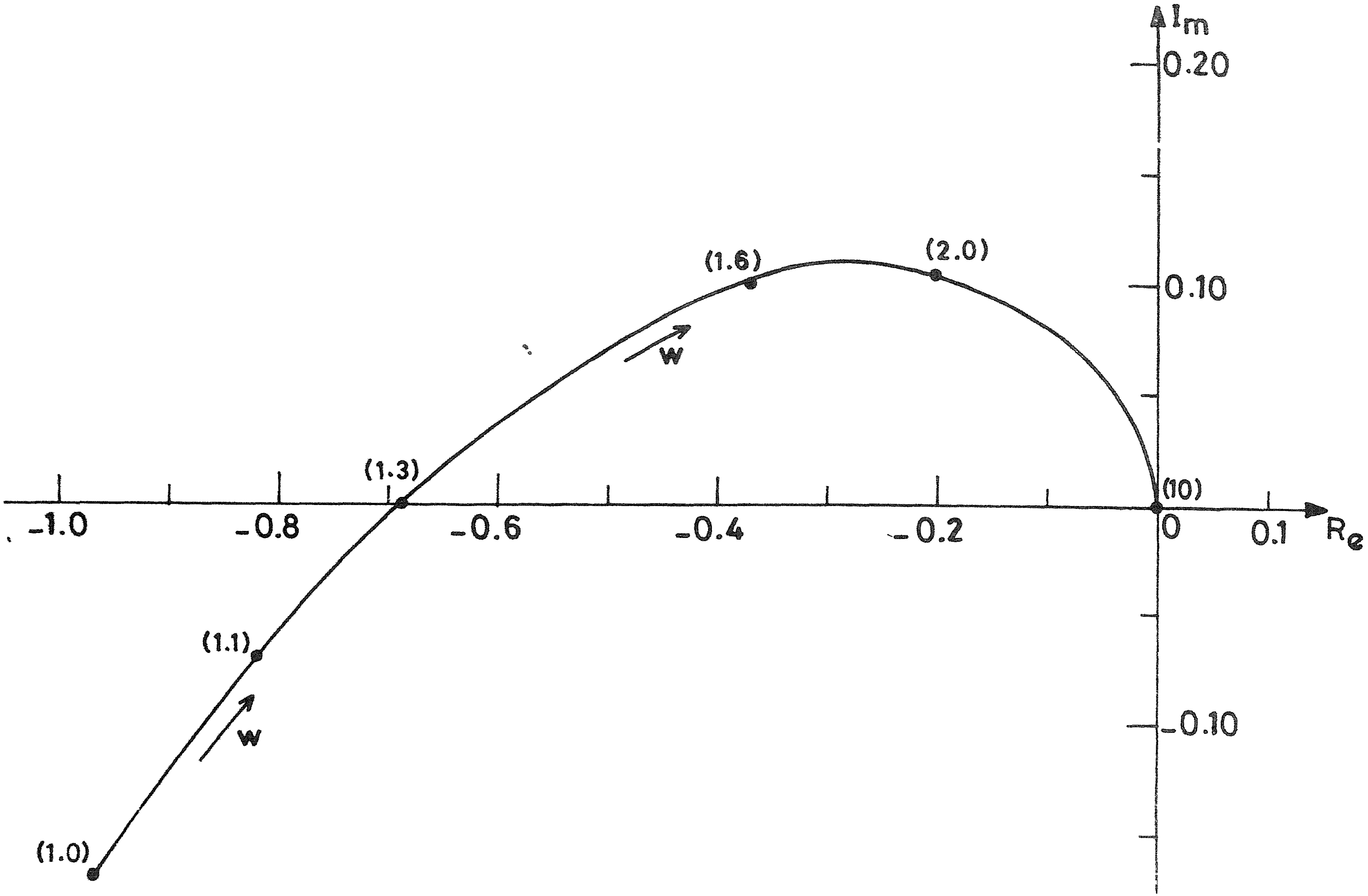

FIG.3.2 FREQUENCY RESPONSE FOR CASE 2 OF TABLE [3.1].

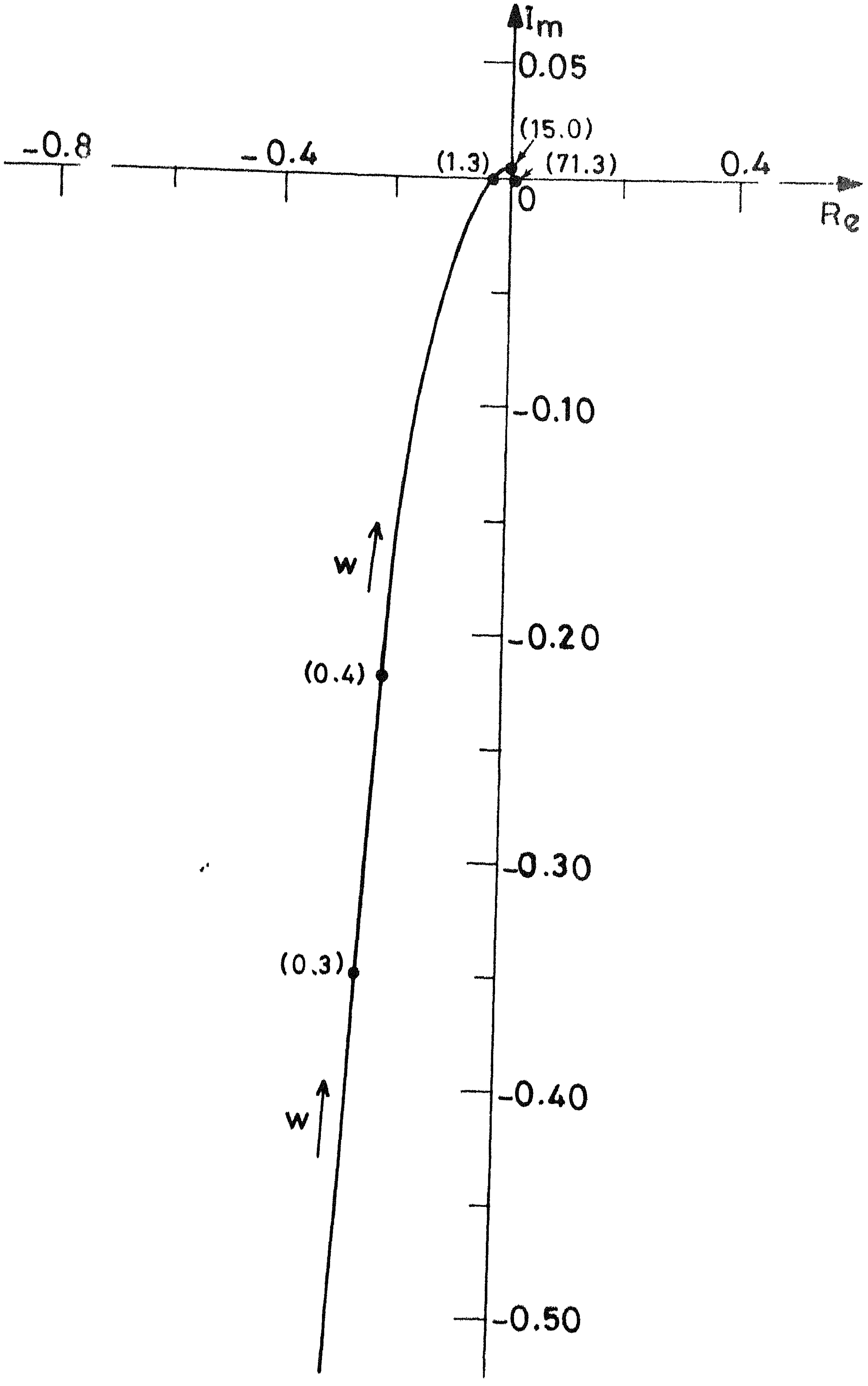

FIG.3.3 FREQUENCY RESPONSE FOR CASE 4 OF TABLE [3.1].

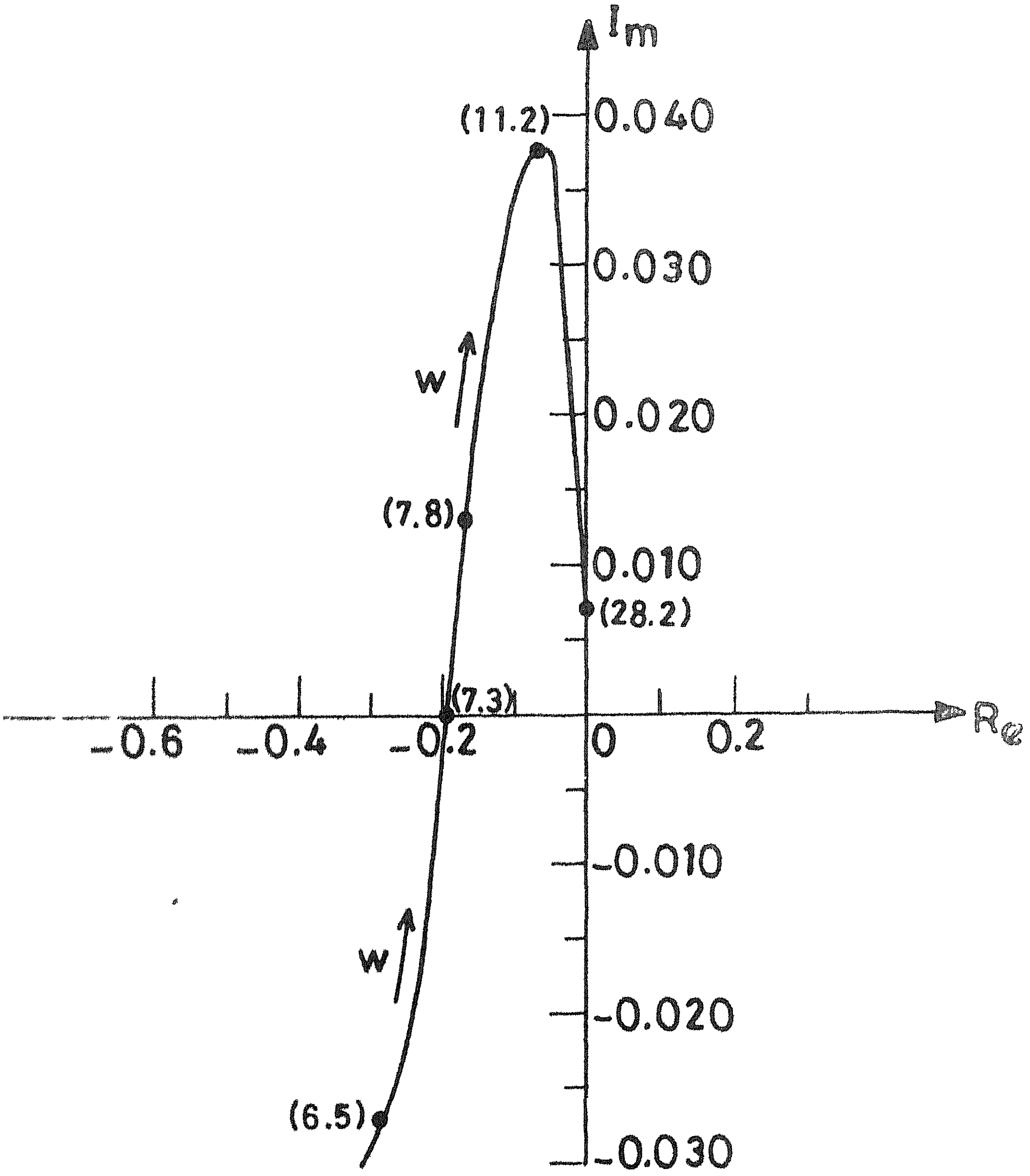

FIG. 3.4 FREQUENCY RESPONSE FOR CASE 6 OF TABLE [3.1].

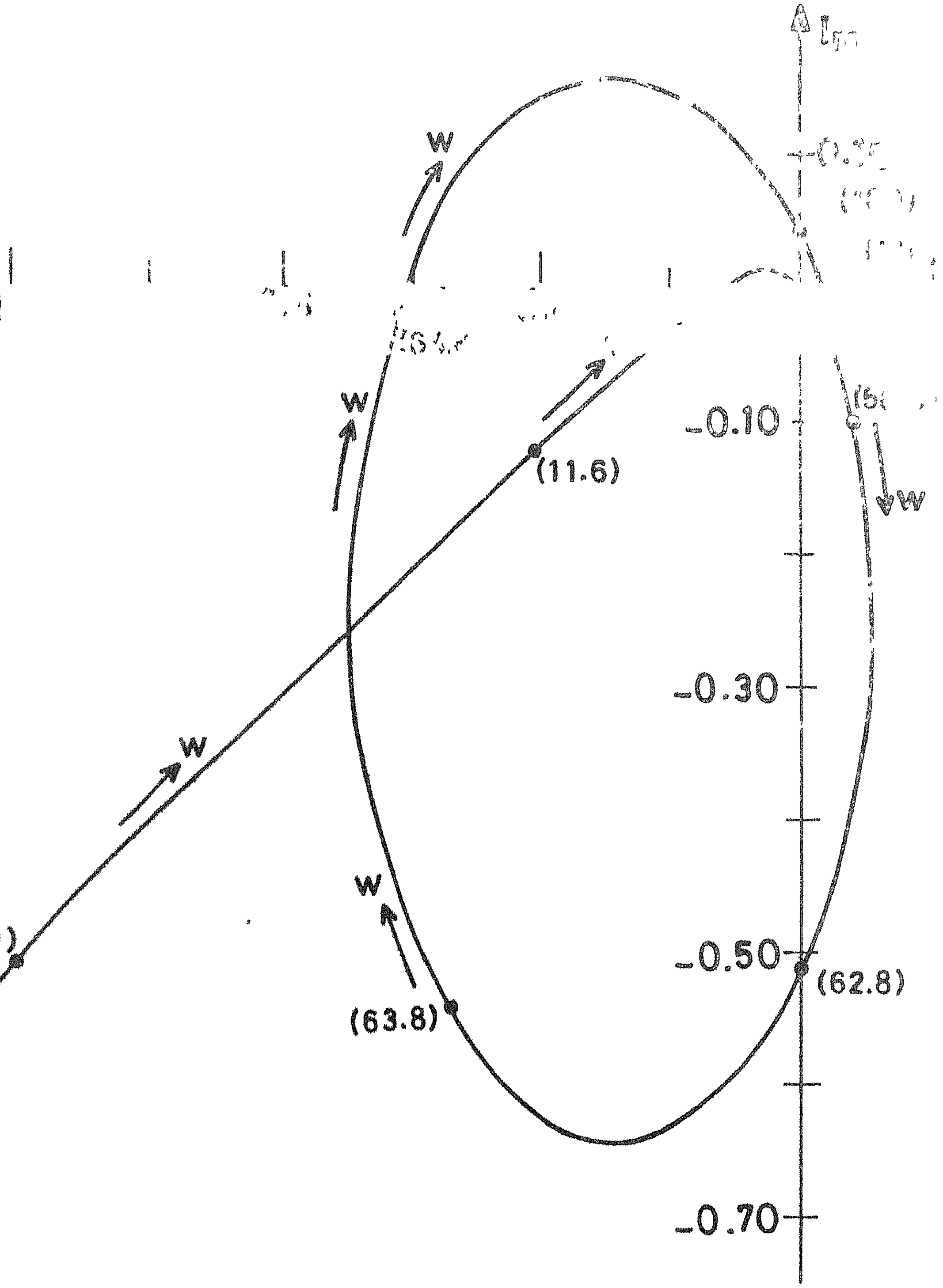

G.3.4(a) FREQUENCY RESPONSE FOR CASE 4 OF TABLE [3.2] in the rectifier controller gain time constant plane and are plotted in Figure 3.5 as curves 1 to 6 for cases 1 to 6 of Table 3.1 respectively. The portion to the left of the boundary is stable, while that on the right is unstable.

A comparison of curves 1 and 2 indicates that with predictive type of C.E.A. controller at inverter, the stability margin at lower time constants is better with EPC at rectifier, while at higher time constants IPC at rectifer is preferable. A similar observation was made in the case of single converter system discussed in the previous chapter and can also be made through comparison of curves (3,4) and (5,6). All these cases in general indicate that the use of EPC at rectifier enhances the stability domain in the range of time constant below 0.1 second.

With rectifier under IPC firing scheme, it is evident from curves 1 and 3 that use of IPC at inverter enhances the stability region significantly at higher time constants. The stability domain is further improved with EPC at the inverter (Figure 3.5).

From comparison of curves (1,2), (3,4), (5,6) and the stability boundary for single converter case (Figure 2.6),

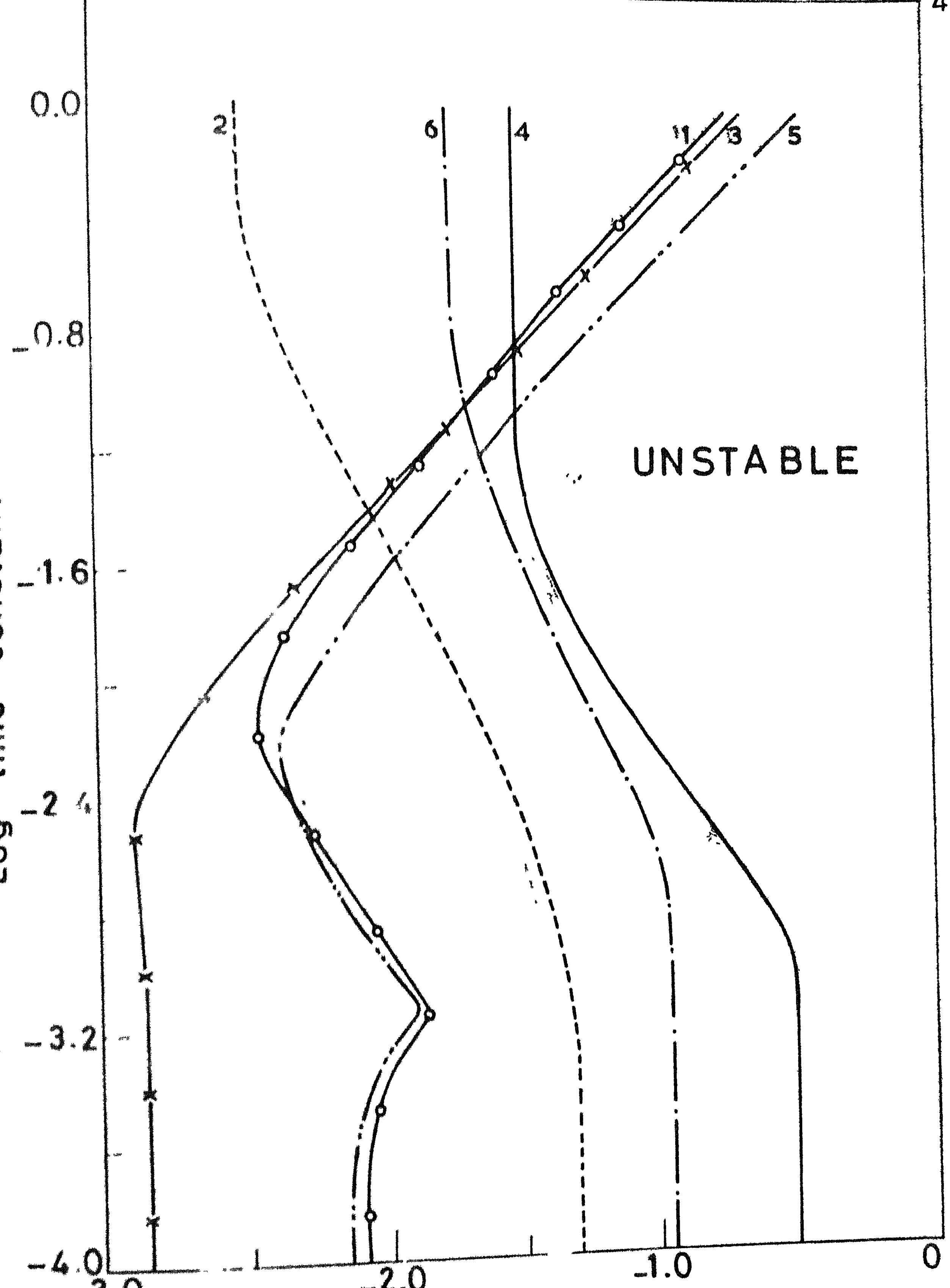

FIG. 3.5 EFFECT OF FIRING SCHEME. STABILITY BOUNDARIES FOR TABLE [3.1].

it is interesting to note that the choice of firing control scheme at the rectifier largly governs the stability characteristics of the system. While with IPC at rectifier, it is evident that controllers parameters can be varied over a wide range. The choice is restricted considerably with EPC at rectifier. Furthermore, comparison of curves 2,4 and 6 indicates that with rectifier under EPC, it is beneficial to have inverter under IPC.

3.3 EFFECT OF CONTROL STRUCTURE

An attempt is made to investigate the stability of the two terminal HVDC system with different control structure. The various cases studied are given in Table 3.2. Rectifier terminal is under constant current control and the inverter is under C.E.A. control. The system parameters and operating conditions are given in Appendix [A-2] .

Figure 3.4(a) shows the frequency response for case 4 of Table 3.2. The oscillations are observed to occur at 25 Hz and 64.8 Hz. Comparison of the responses shown in Figures 3.4(a) and Figure 3.2 for case 2 of Table 3.2 (which is same as case 2 of Table 3.1); shows considerable increase in the frequency at which oscillations can occur leading to system instability. This effect can possibly be attributed to the PI controller, which is incorporated in the system.

A more rigourous comparison of the various cases studied is made on the basis of the stability boundaries plotted in Figure 3.6 for Table 3.2, as curves 1 to 6 for cases 1 to 6 respectively. Comparison of the cases 1 and 3 shows that the stability domain is reduced considerably with the use of the PI controller (case 3), except in the small range of time constant (between 0.01 and 0.001 Second). A similar observation can be made through comparison of curves 2 and 4. It is also observed from curves 3 and 4, that use of EPC at rectifier, improves the system stability significantly with inverter under predictive control. Comparison of curves 1 and 2 (as was done in the previous section) shows that EPC is better only in the lower range of time constant. It is interesting to note from curves (4 and 6) that use of EPC at inverter considerably improves the system stability. A similar effect is evident from comparison of curve (3 and 5) at lower values of time constant.

3.4 EFFECT OF POWER CONTROL AT RECTIFIER

Rectifiers are invariably assigned the task of controlling the dc link power. The effect of power control

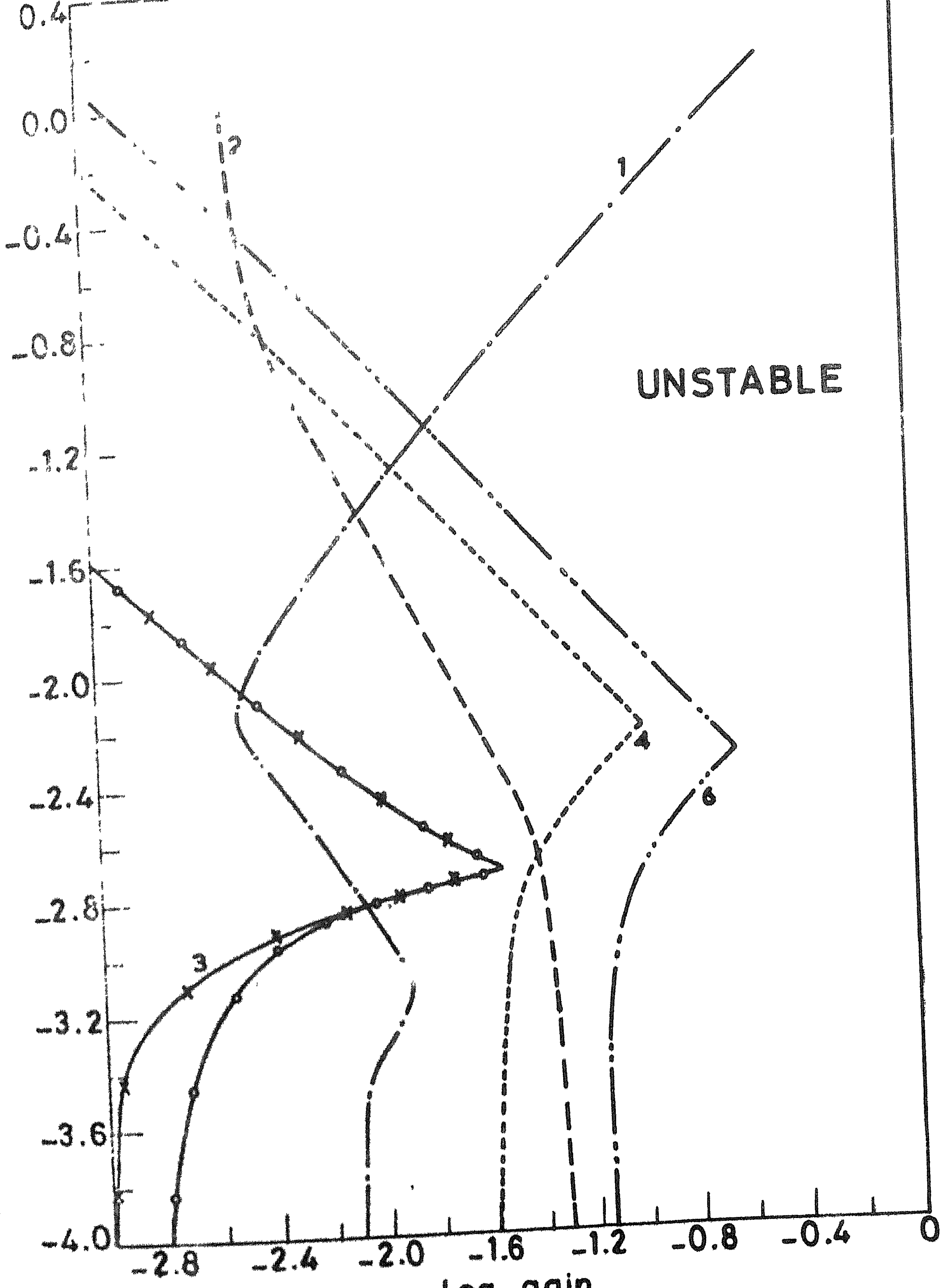

FIG. 3.6 EFFECT OF CONTROL STRUCTURE. STABILITY BOUNDARIES FOR TABLE [3.2]

at rectifier is therefore investigated under both IPC and EPC firing control schemes. The cases studied are given in Table 3.3. The stability boundaries are plotted in Figure 3.7. Comparison of these with curves 1, 2 of Figure 3.5 (corresponding to the current control at rectifier) **does not indicate** any appreciable change in the stability characteristics of the system [17].

3.5 SYSTEM STABILITY WITH INVERTER UNDER CONSTANT β CONTROL

Considering constant β operation of the inverter with IPC and rectifier under current control with IPC, the system stability is investigated with the operating condition as given in Appendix [A-2] ; and the stability domain is plotted in Figure 3.8. For the sake of comparison, the stability boundary for case 3 of Table 3.1 is also shown in Figure 3.8. The development of system model under constant β mode of operation at inverter is given in Appendix [C-2].

It is observed that constant β operation of inverter has a favourable influence on the stability characteristics of the system. This effect may be attributed to the fact that with the constant β operation of the inverter the slope of the dc voltage - dc current characteristic of the inverter becomes positive and thus may lead to better system stability.[3,17].

TABLE 3.3

Cases for Effect of Power Controller

S.No.	Rectifier		Inverter	
	Control	Firing	Control	Firing
1	$[\frac{1}{1+ST_1}].$ $[\frac{-K}{1+ST_2}]$	IPC	-	Predictive
2	"	EPC	-	Predictive

TABLE 3.4

Cases for Effect of Source Inductances

S.No.	Rectifier		Inverter	
	Control	Firing	Control	Firing
1	$[\frac{-K}{1+ST}]$	IPC	$[\frac{-K}{1+ST}]$	IPC
2	"	"		EPC
3	"	EPC		IPC
4	"	"		EPC

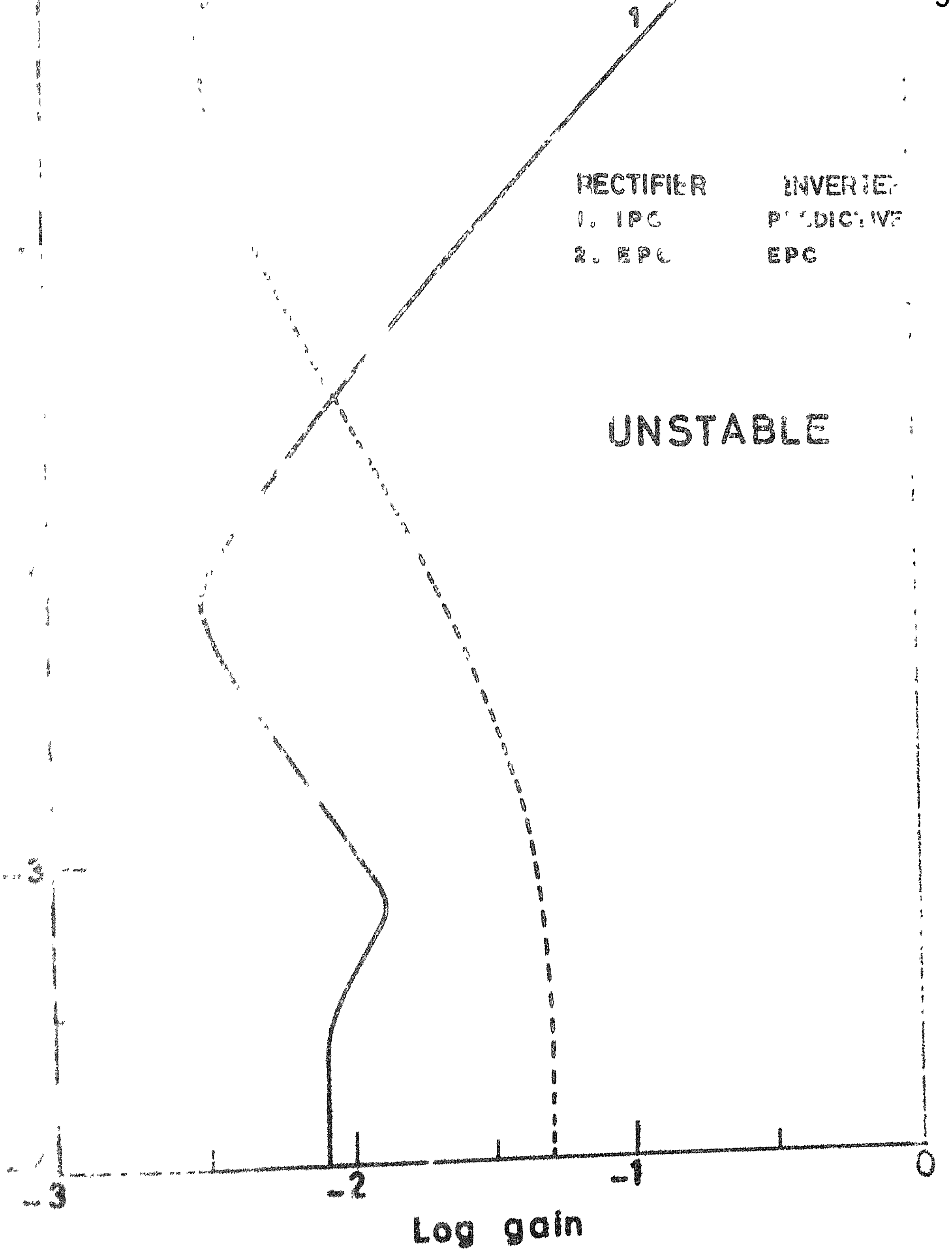

FIG. 3.7 EFFECT OF POWER CONTROLLER. STABILITY BOUNDARIES FOR TABLE [3.3]

87566

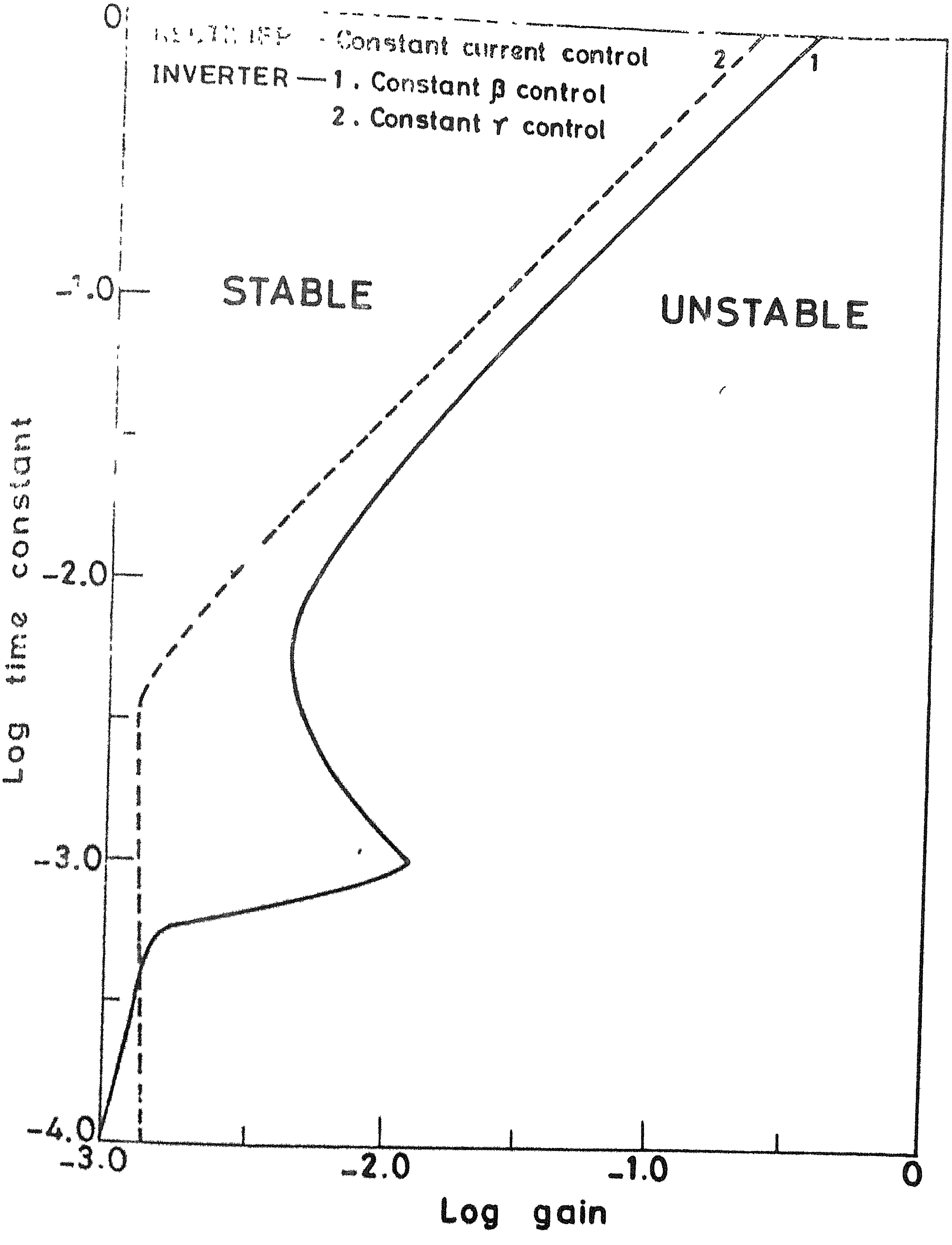

FIG. 3.8 STABILITY BOUNDARIES FOR CONSTANT β - CONTROL.

3.6 EFFECT OF VARIATION IN SYSTEM PARAMETERS

The stability characteristics of the system are investigated with variation in the source inductance at both rectifier and inverter ends and also for variation in transmission line length. Operating conditions for both the cases are restablished accordingly with change in system parameters. For this purpose the rectifier is assumed to be under current control and inverter under constant extinction angle control.

Variation in source inductances at both rectifier and inverter ends are discussed first. The various cases studied are given in Table 3.4 and the stability boundaries are plotted in Figure 3.9. The portion to the left of the boundary is unstable while, that on the right is stable. It is observed that for a given value of source inductance at rectifier end, increase in the value of source inductance at inverter is determental to system stability. However for a given value of source inductance at inverter, increase in source inductance at rectifier has a favourable influence on system stability. Comparison of curves (1 and 2) shows that the EPC firing scheme considerably improves the system stability as opposed to IPC firing scheme. A similar effect of EPC firing scheme is observed through comparison of curves 3 and 4.

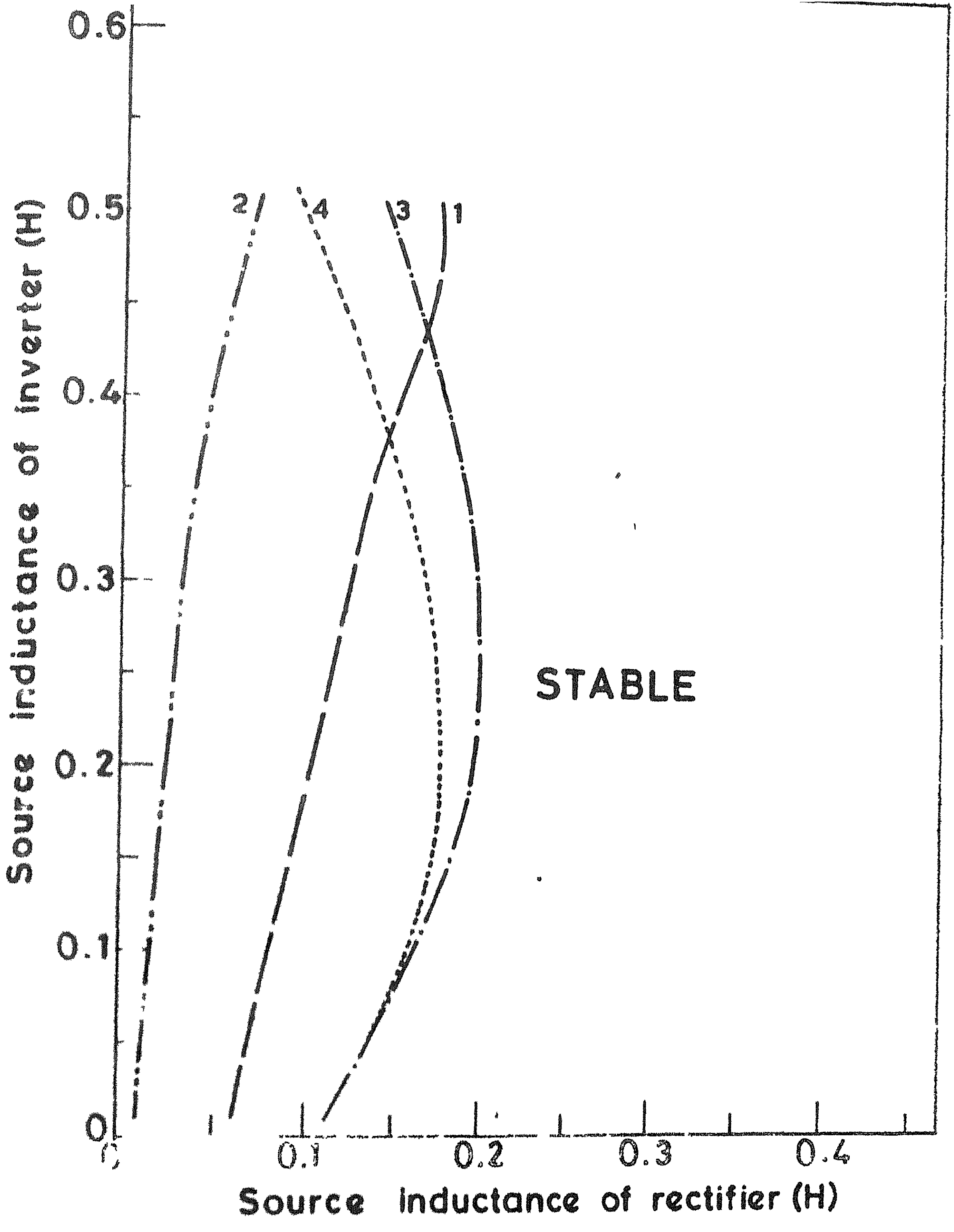

FIG. 3.9 EFFECT OF SOURCE INDUCTANCE. STABILITY BOUNDARIES FOR TABLE [3.4]

The effect of variation in transmission line length and inverter end source inductance on system stability is also studied for the cases given in Table 3.5. The stability domains are plotted in Figure 3.10. The region to the left of the boundary is unstable. It is observed from the various stability boundaries, that for a given inverter end source inductance, there is a minimum transmission line length, which is needed for stable system operation. From curves 1 and 3 it is clear that increase in source inductance should be accompanied with the increase in the transmission line length. This effect is possibly due to the EPC firing scheme at rectifier. However, it is interesting to note that with the use of IPC at rectifier (curve 2), a decrease in the transmission line length should be accompanied by increase in source inductance at inverter end to ensure stable system operation.

Effect of variation of extinction angle was also observed at inverter end. The operating conditions were recalculated for this variation to maintain a constant dc current. Considering rectifier under constant current control with IPC and inverter under constant extinction angle control with IPC, the stability domains are obtained for different values of extinction angles. These are plotted in Figure 3.11 in the plane of rectifier and inverter controller gains. It

TABLE 3.5

Cases for Effect of Transmission Line Length

S.No.	Rectifier		Inverter	
	Control	Firing	Control	Firing
1	$\left[\frac{-K(1+ST_1)}{1+ST_2}\right] \cdot \left[\frac{1+S}{S}\right]$	EPC	-	Predictive
2	"	IPC	$[-K]+\left[\frac{1+S}{S}\right]$	EPC
3	"	EPC	"	EPC

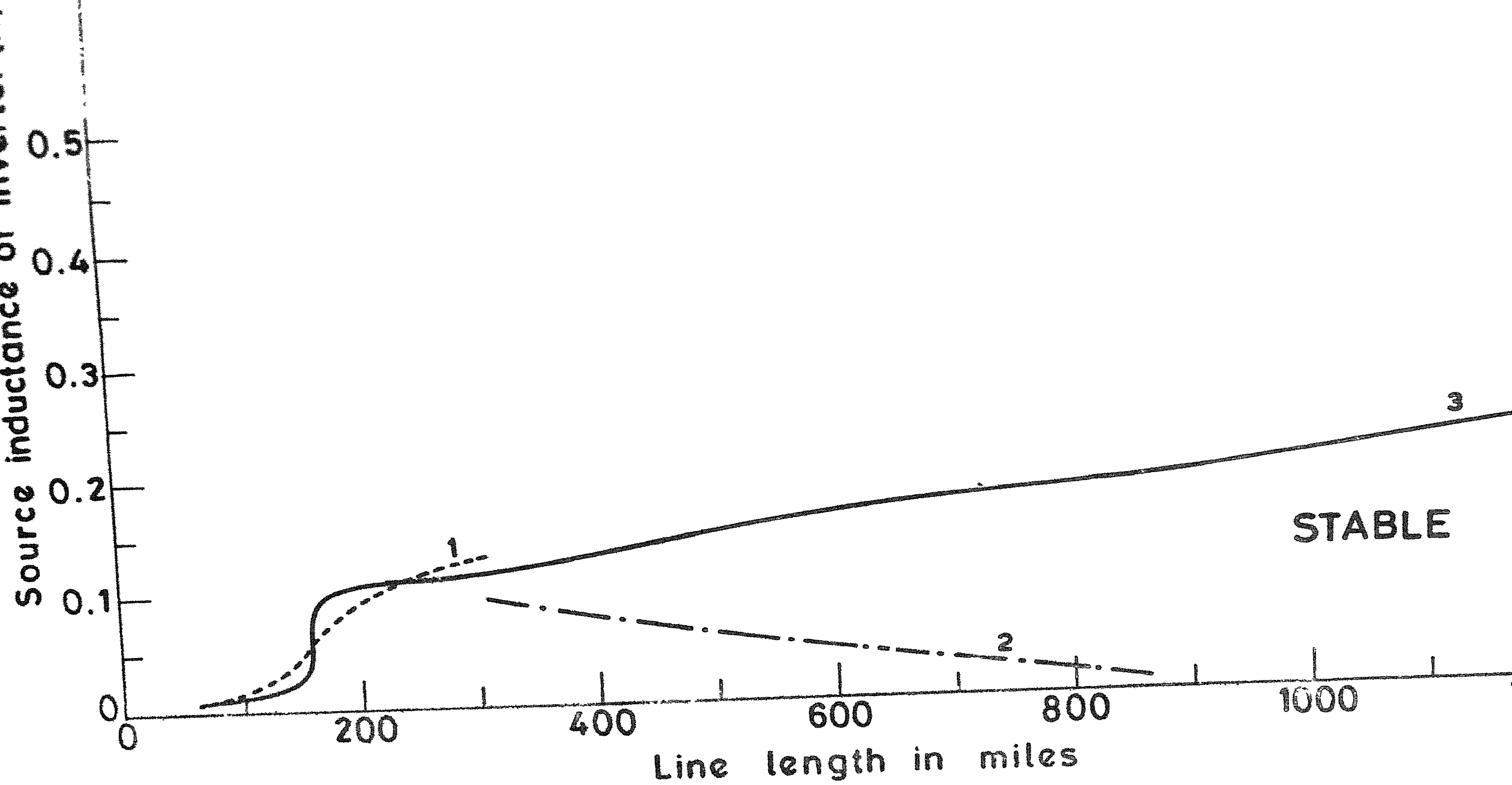

FIG.3.10 EFFECT OF TRANSMISSION LINE LENGTH.
STABILITY BOUNDARIES FOR TABLE [3.5].

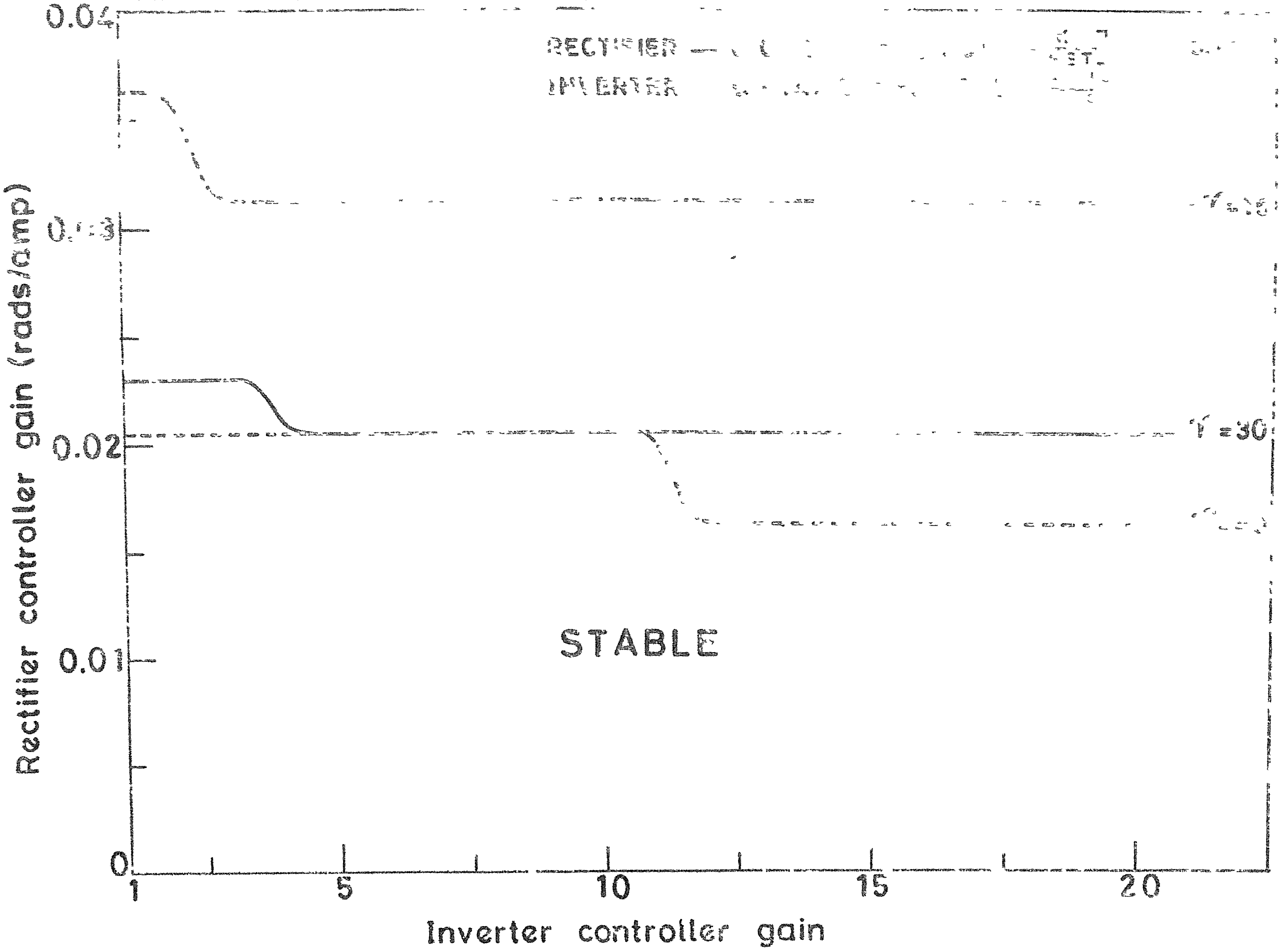

FIG. 3.11 EFFECT OF EXTINCTION ANGLE.

can be observed that increase in the extinction angle is determental to system stability. A similar effect of increase in extinction angle has been reported in [16].

3.7 CONCLUSION

A general model for representation of two terminal HVDC system is developed in detail. This model is flexible to accomodate changes in structure of different subsystems involved in it. Various cases are studied to observe the influence of firing control scheme, controller-structure, control-strategy and system parameters. Inferences drawn from there studies are found to be in agreement with reported literature to a great extent.

CHAPTER 4

TWO TERMINAL HVDC SYSTEM STABILITY WITH DIODE BRIDGE RECTIFIER

In a HVDC system, whether two terminal or multi-terminal, one of the terminals operate under voltage control, defining the voltages on the dc system buses. In ref[18] Bowles has reported that a reliable voltage control can be obtained in HVDC system by using a diode bridge in place of conventional thyristor bridge at rectifier station particularly when the generation is isolated.

In a two terminal HVDC transmission schemes under operation, the inverter terminal operates with constant extinction angle thereby controlling the system voltage. Use of diode bridge converter as an inverter is not very feasible due to the problem of commutation failure.[18].

In this chapter, the stability characteristic of a two terminal HVDC system with a diode bridge converter as a rectifier terminal is investigated. The inverter terminal is chosen to operate under constant current control. The system model is developed employing the component models given in Chapter 2. Stability is then analysed based on eigen value criterion.

4.1 MODEL FORMULATION

In a diode bridge, the firing always takes place at the positive going zero crossing of the commutation voltage thus resulting in zero delay angle. Converter equation (2.9) at rectifier can, therefore, be modified suitably and written as

$$V_{dR}(K) = \frac{1}{\Delta t_K}[\,0 - 2L_c\,\Delta I_{dR}(K+1) + L_C\,\Delta I_{dR}(K)\,] \qquad \text{-- (4.1)}$$

Furthermore, a current control is realised at inverter alongwith IPC firing control scheme. The continuous time equation for this is

$$\Delta \dot{\underline{X}}_C = [A_C]\Delta \underline{X}_C + \underline{B}_C \;\; \Delta U_{diode}(K) \qquad \text{-- (4.2)}$$

$$A_C = \begin{bmatrix} -\frac{1}{T_1} & 0 \\ 0 & -\frac{1}{T_1} \end{bmatrix} ; \underline{B}_C = \begin{bmatrix} -K_1/T_1 \\ 0 \end{bmatrix} \quad ; \Delta U_{diode}(K) = \Delta I_{dI}$$

where K_1 and T_1 are the gain and time constant of controller. Equation (4.2) is then combined with the transmission line equation (2.10) to give overall continuous time equation as

$$\Delta \dot{\underline{X}} = [A]\Delta \underline{X} + [B]\;\; \Delta \underline{V}_{dc}(K) \qquad \text{-- (4.3)}$$

The above equation is then discretized as discussed in Appendix [B] to give

$$\underline{X}(K+1) = e^{[A]\;\;\Delta t_K}\Delta \underline{X}(K) + [MD]\,[B]\Delta \underline{V}_{dc}(K) \quad \text{-- (4.4)}$$

Equation for converter dc voltage is

$$\Delta \underline{V}_{dc}(K) = \frac{\Delta \underline{U}_{DC}(K)}{\Delta t_K}$$

where $\Delta \underline{U}_{DC}(K) = [A_1]\,\Delta\alpha(K) + [A_2]\,\Delta\underline{X}(K+1) + [A_3]\,\Delta\underline{X}(K)$

-- (4.5)

$$\text{where } [A_1] = \begin{bmatrix} 0 & 0 \\ 0 & \dfrac{-\sqrt{2}E\ \text{Sin}\ \alpha\, I_o}{w_o} \end{bmatrix} ; [A_2] = \begin{bmatrix} -2L_C & 0 \\ 0 & -2L_C \end{bmatrix}$$

$$\text{and} \quad [A_3] = \begin{bmatrix} L_C & 0 \\ 0 & L_C \end{bmatrix}$$

Equations (4.4) and (4.5) are combined with following equation for firing pulse generators.

$$\Delta \underline{\alpha}(K) = \begin{bmatrix} 0 \\ K_{fs} \end{bmatrix} \Delta V_C \qquad \text{-- (4.6)}$$

where V_C is the control voltage, obtained from controller output at inverter end and sent to corresponding firing pulse generator whose gain is K_{fs}.

Thus the overall system model is represented as

$$\Delta \underline{X}'(K+1) = \left[AA\right]\Delta \underline{X}'(K) + \underline{BB}\ \Delta V_C(K) \qquad \text{-- (4.7)}$$

A closed loop matrix is thereafter obtained to analyse the system stability as discussed in section 2.6 for single converter system.

4.2 RESULTS

The stability study is carried out with the operating conditions and system parameters as given in Appendix [A-3] . Stability boundary is plotted in the plane of gain and time constant of the current controller in Figure 4.1. Comparison of the system discussed in this chapter is made with the conventional systems having thyristor bridges at both the rectifier and inverter corresponding to cases 3 and 4 of Table 3.1. A drastic improvement in stability domain is observed with the system having diode bridge.

4.3 CONCLUSION

This chapter demonstrates the desirability of having a diode bridge at rectifier. The study is carried out for

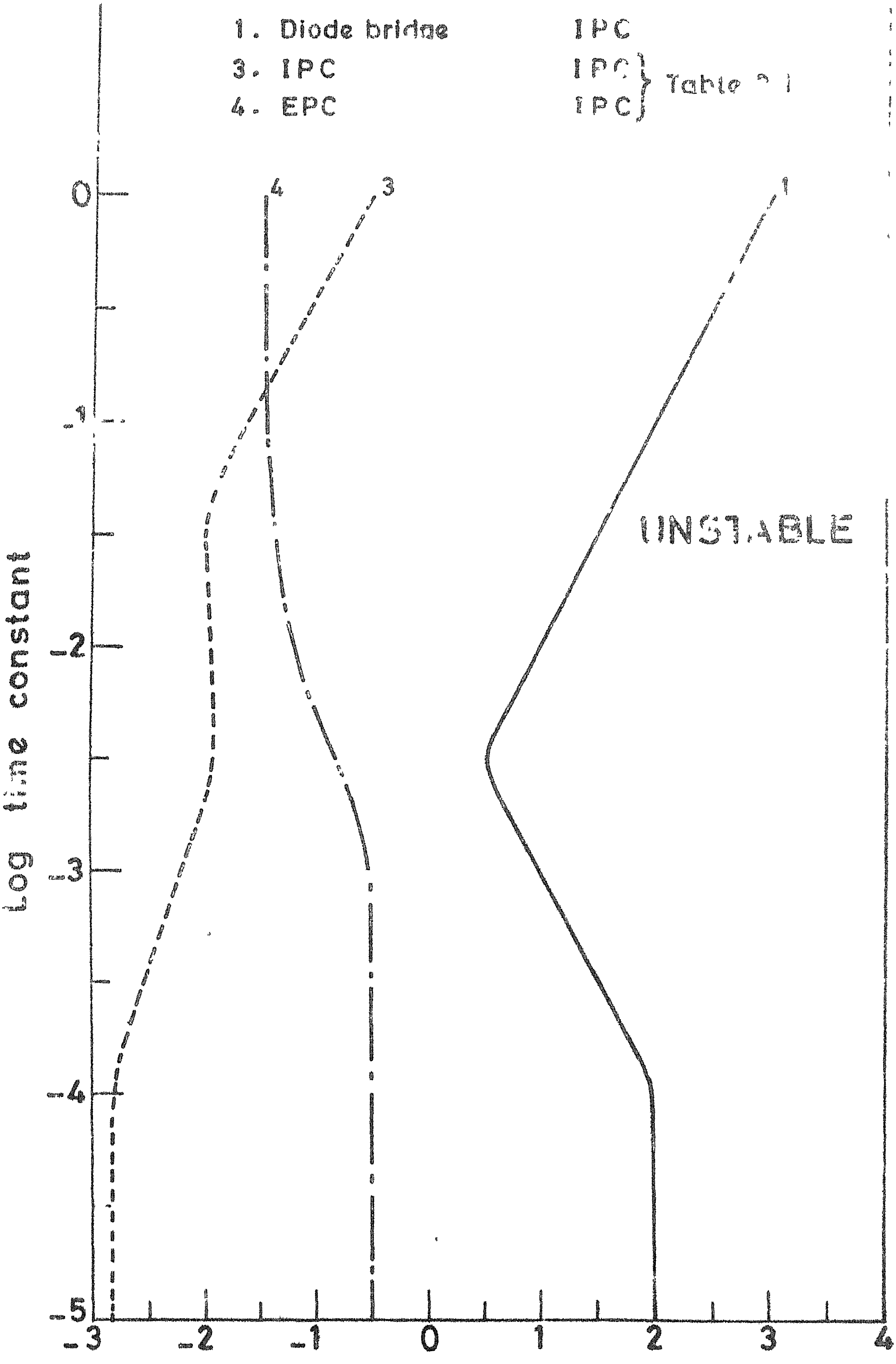

FIG. 4.1 STABILITY BOUNDARIES FOR DIODE BRIDGE

two terminal system, however, it is found that the scheme is also suitable for multiterminal systems also having remote generation [12]. For the case studied, it is observed that there is a major improvement in the stability characteristics of the system with diode bridge rectifier.

CHAPTER 5

CONCLUSION

5.1 OPERATING POINT STABILITY ANALYSIS

With the rapid developments in the HVDC transmission technology, attempts are being made to improve the system performance through use of better control alternatives even in the case of existing two terminal HVDC installations whose operation is fairly well established now. This, therefore, stresses the need to have a systematic approach for the design of converter control system to ensure reliable system operation. In this context the operating point stability analysis of two terminal HVDC system has been attempted in this thesis. The formulation of the HVDC system model proceeds with the development of the individual component models, constituting the HVDC system, and their interconnection through appropriate system variables.

The discrete time representation of the converter based on average system quantities is reported in Chapter 2 alongwith the development of the component models for DC transmission line, converter control and firing pulse generator. The interconnection of these subsystem models through appropriate interfacing variables leads to the linearised, discrete time, state space description of the overall system as discussed in Chapter 3. The system stability is investigated using linear control theory techniques in both frequency and time domain (eigen value analysis). The approach for the formulation of the system model is extremely modular in nature and therefore enables dynamic representation of the various subsystems to any desired degree of detail.

The system model is employed to investigate the stability characteristics of the two terminal HVDC system with both Individual phase control and Equidistant pulse control firing schemes. One of the features of the study is to investigate the performance of a feedback type of extinction angle controller at the inverter under both IPC and EPC firing control schemes. It has been observed that use of EPC firing scheme at inverter helps to improve the system stability when the source inductance is large. The results of the various case studies reveal that the choice of IPC or EPC scheme at either rectifier or inverter terminals is dependent to a great extent on the system parameters. It has also been observed that the constant β (advance angle) operation of the inverter led to a better stability margin as compared to the constant extinction angle operation. Although this result is as expected, but constant β operation is not generally considered at the inverter due to the problem of commutation failure and may be useful only in certain specific system conditions.

The possibility of using a diode bridge converter, in place of the conventional thyristor converters at the rectifier terminal has been reported in the literature particularly when the generation is remote. The study of the stability characteristics of the system with this alternative has been reported in Chapter 4 and it reveals that use of diode bridge converter at rectifier station drastically improves the system stability.

The stability investigations undertaken in this thesis may be considered as a first step towards the final selection of the controller parameters which in turn, has to be made through detailed study using digital simulation or HVDC simulator.

5.2 SCOPE FOR FURTHER WORK

1. In the study reported in this thesis, the effect of the ac system dynamics is neglected under the assumptions of strong ac system. However, in case of HVDC links connec-

ted between weak ac systems, the interaction between the ac and dc system dynamics influences the performance of HVDC system to a considerable extent. It will, therefore, be necessary to include representation of the ac system in the stability analysis for the purpose of controller design.

2. Since the multiterminal HVDC systems are being planned for the future, it is necessary to analyse the system stability for the proper design of the coordinated control systems.

3. The studies reported in the thesis are confined to the systems employing analog control techniques. However, with increasing interest in the use of microprocessor control, it would be interesting to study the system stability characteristics with digital control strategies.

APPENDIX A

OPERATING CONDITIONS AND SYSTEM PARAMETERS

A-1 Single Converter System

No Load DC Voltage = 100 Volts

Direct Current = 5 Ampere

Commutating Inductance = 0.005 H

Firing angle = 15°

Load resistance = 17.818 ohms

Load time constant = 0.2 Second

Frequency = 50 Hz

Except for T_2 all other values are taken from [11]

A-2 Two Terminal HVDC System

Rated dc link power = 906 Mw

Frequency = 60 Hz

AC line voltage at rectifier end = 525 kV

AC line Voltage at inverter end = 500 kV

DC current = 726 Ampere

Commutating inductances for rectifier and inverter = 0.09 H

Line resistance = 0.0508 ohm/mile

Line capacitance = 0.0091 μF/mile

Line inductance = 0.00324 H/mile

Line length = 800 miles

Smoothing reactor resistance = 1.87 ohm

Smoothing reactor inductance = 0.5 H

For the Cases reported in Table 3.1

Rectifier firing angle = 15.46°, Extinction angle = 15°.

(i) Frequency Response (Figs. 3.1, 3.2, 3.3, 3.4)

Case 1 : At rectifier K = 0.0343 rad/amp, T = 0.2S

Case 2 : At rectifier K = 0.0025 rads/amp, T = 0.2S

Case 4 : At rectifier K = 0.01 rads/amp, T = 0.2S

At Inverter K = 0.0343 rads/amp, T = 0.2S

Case 6 : At rectifier K = 0.01 rads/amp, T = 0.2S

At Inverter K = 0.0343 rads/amp, T = 0.2S

(ii) Stability Boundaries (Fig. 3.5)

For all the case where feedbak type of CEA control is considered at inverter, K = 0.0343, T = 0.2S

For the Cases reported in Table 3.2

Rectifier firing angle = 15.46°, Extinction Angle = 15°

(1) Frequency Response (Fig. 3.4a)

Case 4 : At rectifier K = 0.0343 rads/amp, T_1 = 0.01S, T_2 = 0.005S

(ii) Stability Boundaries (Fig. 3.6)

The stability boundaries for cases 3,4,5 and 6 are plotted in the K-T_2 plane of the controller at the rectifier terminal which is of the type $\frac{-K(1+ST_1)}{(1+ST_2)} \cdot (\frac{1+S}{S})$.

T_1 was chosen as 0.01S

For cases 5 and 6, the inverter controller gain is

K = 0.0343

For the cases reported in Table 3.3

Rectifier firing angle = 15.46°, Extinction angle = 15°.

At rectifier T_1 = 0.01S

The stability boundaries are plotted in the K-T_2 plane (Fig. 3.7).

For the cases reported in Table 3.4

Rectifier terminal dc current = 726 Amps

Inverter extinction angle = 15°

Rectifier and Inverter Side Controller parameters = K = 0.0343, T = 0.2S

The rectifier and inverter firing angles were calculated with change in source inductances.

For the cases reported in Table 3.5

At rectifier K = 0.003

T_1 = 0.00316S

T_2 = 0.005S

At Inverter (Cases 2 and 3) : K = 10.0

The rectifier and inverter firing angles were calculated with variation in inverter side source inductance and transmission line length.

With Constant β Control at Inverter

Rectifier firing angle = 15.46°

Inverter firing angle = 153.65°

At Inverter K = 0.0343, T = 0.2S

Stability boundary is plotted in the plane of controller parameters at rectifier.

A-3 Two Terminal HVDC System with diode bridge Rectifier

System Parameters are same as given in Appendix A-2. Rectifier terminal had no control

Inverter terminal was equipped with Feedback type of Current Control $[K/(1+ST)]$: K = 0.0343 rad/amps and T = 0.2S . Inverter firing angle = 153.65°. Stability boundary was plotted in the K-T plane of the inverter controller.

APPENDIX B

DISCRETIZATION OF CONTINUOUS TIME STATE EQUATION

Consider a continuous time equation

$$\dot{\underline{X}} = [A]\,\underline{X} + [B]\,\underline{u} \qquad \text{-- (B.1)}$$

The solution of this equation is

$$\underline{X}_{(t)} = e^{[A]\,t}\,\underline{X}_{(o)} + e^{[A]\,t} \int_0^t e^{-[A]\,\tau}\,[B]\,u(\tau)\,d(\tau) \qquad \text{-- (B.2)}$$

Assuming the forcing function to maintain a constant value of $u_t(K)$ during the interval of time from the instant $t(K)$ to $t(K+1)$, [5].

$$\underline{X}(K+1) = e^{[A]\Delta t_K}\,\underline{X}_t(K) + \left\{ \int_{t(K)}^{t(K+1)} e^{A\,(t(K+1)-\tau)}\,d\tau \right\} [B]\,\underline{u}_t(K) \qquad \text{-- (B.3)}$$

where $\Delta t_K = t(K+1) - t(K)$

If $t(K+1) - \tau = t'$, then

$$\underline{X}_t(K+1) = e^{[A]\Delta t_K}\,\underline{X}_t(K) + [MD]\,[B]\,\underline{u}\;\; t(K) \qquad \text{-- (B.4)}$$

where $[MD] = \int_0^{t_K} e^{[A]\,t'}\,dt'$

$$= \Delta t_K \left\{ [\,1\,] + \frac{[A]\ \Delta t_K}{\lfloor 2} + \frac{[A]^2\ \Delta t_K^2}{\lfloor 3} + \ldots\ldots \right\} ;$$

when $[A]$ is singular -- (B.5)

$$= \left\{ e^{[A]\ t_K} - [\,I\,] \right\} \quad [A]^{-1} ;$$ when $[\,A\,]$ is nonsingular -- (B.6)

only first few terms of series in (B.5) are considered to find [MD] [2] .

APPENDIX C

MODEL FORMULATIONS

C-1 Controller model for case 6 of Table 3.1-

In the case considered, both the rectifier and inverter are equipped with EPC firing control scheme. The block diagrams for the controllers are shown in Figure (C.1) and (C.2). The controller dynamics can be described as follows.

For rectifier terminal

$$\Delta P = \frac{-1}{T_1} \Delta \underline{P} + \frac{K_1}{T_1} \Delta I_{dR} \qquad \text{-- (C.1)}$$

For Inverter terminal

$$\Delta v_{C2} = -\frac{1}{T_2} \Delta v_{C2} + \frac{K_2}{T_2} \Delta \gamma_m \qquad \text{-- (C.3)}$$

$$\Delta \gamma_m = G1 \ \Delta I_{dI} + G2 \ \Delta \alpha_I \qquad \text{-- (C.4)}$$

Hence $\Delta \dot{v}_{C2} = -\frac{1}{T_2} \Delta v_{C2} + \frac{G_1 K_2}{T_2} \Delta I_{dI} + \frac{G_2 K_2}{T_2} \Delta \alpha_I$ - (C.5)

The equations (C.1) and (C.5) can be written as follows in conformation with equation (2.20) to give the dynamics of controllers as

$$\Delta \dot{\underline{X}}_E = [A_E] \ \Delta \underline{X}_E + [B_E] \ \Delta \underline{U}_E \qquad \text{(C.6)}$$

where $\Delta \underline{X}_E^T = \begin{bmatrix} \Delta P & \Delta v_{C2} \end{bmatrix}$

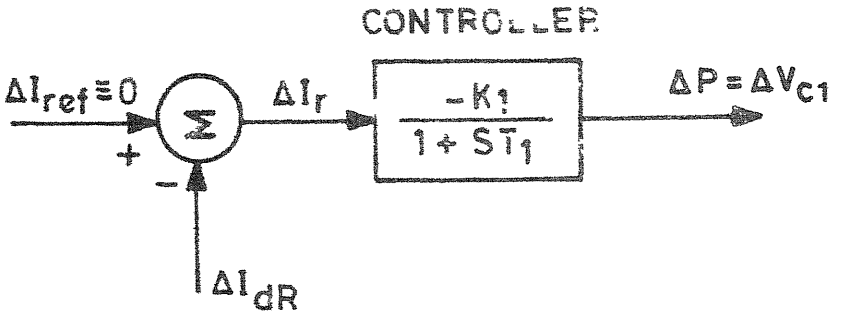

FIG. C-1 CONTROLLER AT RECTIFIER FOR CONSTANT CURRENT.

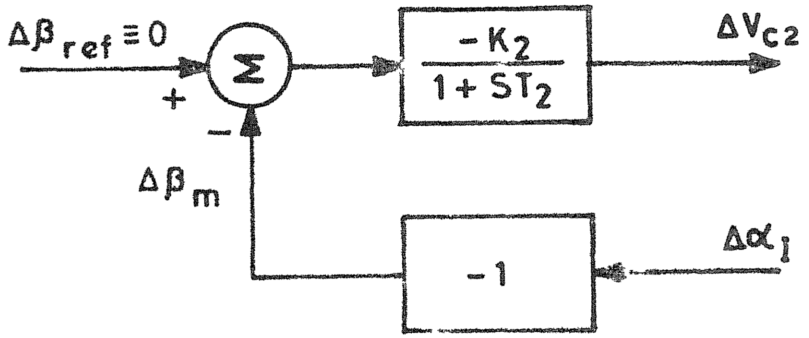

FIG. C-3 CONTROLLER AT INVERTER FOR CONSTANT β.

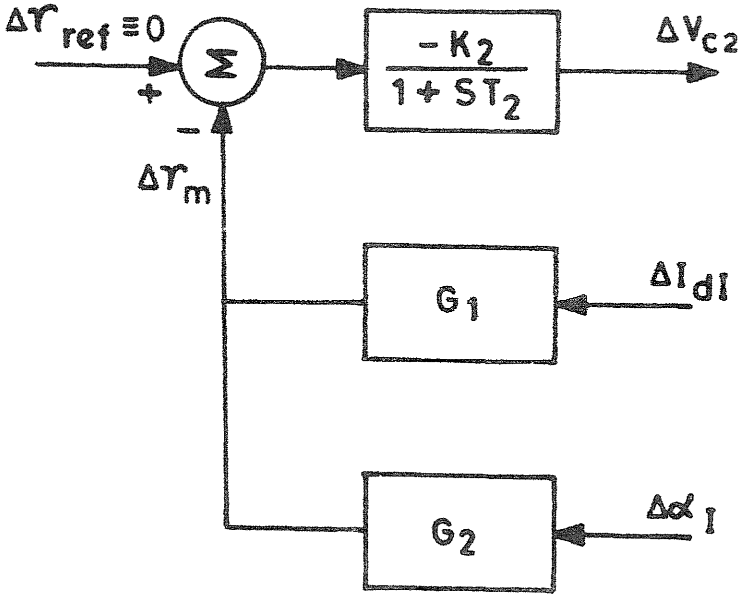

FIG. C-2 CONTROLLER AT INVERTER FOR CONSTANT γ .

and $\Delta \underline{U}_E^T = [\Delta I_{dR} \quad \Delta I_{dI} \quad \Delta \alpha_I]$

Equation (C.6) is then combined with the transmission line equation (2.10) to give

$$\Delta \dot{\underline{X}} = [A]\,\Delta \underline{X} + [B]\,\Delta \underline{U}_d(K) \qquad \text{-- (C.7)}$$

where

$$\Delta \underline{X} = \begin{bmatrix} \Delta \underline{X}_E \\ \\ \Delta \underline{X}_N \end{bmatrix}$$

and

$$\Delta \underline{U}_d^T(K) = [\Delta \alpha_I(K) \qquad \Delta \underline{V}_{dc}^T(K)]$$

The firing angles at the converters are given by

$$\begin{aligned} \Delta \alpha_R(K) &= \Delta Z_1(K) \\ \Delta \alpha_I(K) &= \Delta Z_2(K) \end{aligned} \qquad \text{-- (C.8)}$$

Equation (C.7) is discretized and combined with equations for firing angles (C.8) and converter (3.6, 3.7) to give

$$\underline{X}\ (K+1) = [AA]\ \Delta\ \underline{X}(K) + \underline{BB}\ \Delta V_C(K) \qquad \text{-- (C.9)}$$

Dynamics of VCOs are given by

$$\Delta Z_1(K+1) = \Delta Z_1(K) + K_{fs1}\ \Delta t_K \Delta V_{C1}(K)$$
$$\Delta Z_2(K+1) = \Delta Z_2(K) + K_{fs2}\ \Delta t_K \Delta V_{C2}(K) \qquad \text{-- (C.10)}$$

where K_{fs1} and K_{fs2} are the unity gains of firing pulse generat at rectifier and inverter respectively.

Equations (C.9) and (C.1)) are combined to represent the overall model of the system.

$$\Delta \underline{X}'(K+1) = [A'] \Delta \underline{X}'(K) + \underline{B}'\ \Delta V_C(K) \qquad \text{-- (C.11)}$$

C-2 Constant β Converter-Controller at Inverter -

The block diagrams given in figures (C.2) and (C.3) show the controllers at rectifier and inverter ends. The corresponding equations are

$$\Delta \dot{P} = -\frac{1}{T_1}\ \Delta P + \frac{K_1}{T_1}\ \Delta I_{dR} \qquad \text{-- (C.12)}$$

and $$\Delta \dot{V}_{C2} = -\frac{1}{T_2}\ \Delta V_{C2} - \frac{K_2}{T_2}\Delta\alpha_I \qquad \text{-- (C.13)}$$

The equations can then be combined to give

$$\Delta \dot{\underline{X}}_{CB} = [A_{CB}] \Delta \underline{X}_{CB} + [B_B]\ \Delta \underline{U}_B \qquad \text{(C.14)}$$

where $\Delta \underline{X}_{CB}^{T} = [\Delta P \;\; \Delta V_{C2}]$, $\underline{U}_B$ is the input vector containing rectifier dc current and inverter firing angle.

Equation (C.14) is then combined with the equation of transmission line (2.10) to give

$$\Delta \dot{\underline{X}} = [\,A\,]\Delta \underline{X} + [\,B\,] \;\Delta \underline{U}_d(K) \qquad \text{-- (C.15)}$$

Equation (C.15) is discretized and combined with converter and firing pulse generator equations to give

$$\Delta \underline{X}(K+1) = [\,AA\,]\Delta \underline{X}(K) + \underline{BB} \;\; \Delta V_{C2} \qquad \text{(C.16)}$$

Equation (C.16) describes the constant β controller model

REFERENCES

1. K.R. Padiyar and Sachchidanand, 'Stability of Converter Control for Multiterminal HVDC Systems' 84 T&D 386-9, Paper presented in IEEE/PES 1984 T&D Conference, Kansas City.

2. Sachchidanand, 'Digital Simulation and Stability Analysis of Multiterminal HVDC Systems', Ph.D. Thesis, I.I.T. Kanpur, 1982.

3. Edward Wilson Kimbardk, 'Direct Current Transmission-Vol. I', John Wiley and Sons, (Wiley Interscience), New-York, 1971.

4. Fallside F. and Farmer A.R., 'Ripple Instability in Closed Loop Control Systems with Thyristor Amplifiers', Proc. IEE, 67, 114(1) pp. 139-152.

5. Katsuhike Ogata, 'Modern Control Engineering', Prentice Hall of India 1982.

6. Persson, E.V., 'Calculation of Transfer Functions in Grid-Controlled Converter Systems', Proc. IEE, 70, 117, (5), pp 989-997.

7. Narain G. Hingorani and Philip Chandwick, 'A New Constant Extinction Angle Control for AC/DC/AC Static Converters', IEEE Trans. PAS Vol. 87, no. 3. March 68. pp 866-872.

8. J.D. Ainsworth, 'The phase-locked Oscillator - A New Control System for Controlled Static Converters', IEEE Trans. PAS. Vol. -87 No.3 March 68. pp. 859-865.

9. J.D. Ainsworth, 'Harmonic Instability Between Controlled Static Converters and AC Network', Proc. IEE, Vol. 114, July 67, pp 949-957.

10. A. Ekstrom and Gote Liss, 'A Refined HVDC Control System', IEEE Trans. PAS Vol. 89 No. 5/6 March 70 pp 723-732.

11. J.P. Sucena-Paiva, R. Hernandez and L.L. Freris, 'Stability Study of Controlled Rectifiers Using a New Discrete Model', Proc. IEE, Vol. 119, No. 9 - Sep. 72 pp. 1285-1293.

12. J.P. Sucena-Paiva and L.L. Freris, 'Stability of a d.c. Transmission Link Between Weak a.c. Systems :, Proc. IEE, Vol. 121, No.6, June 74. pp 508-515

13. J.P. Sucena-Paiva and L.L. Freris, 'Stability of Rectifiers with Voltage Controlled Oscillator Firing Systems', Proc. IEE, Vol. 120, No. 6. June 73 pp. 667-673.

14. J.P. Sucena Paiva, 'Stability of a d.c. Transmission Link Between Strong a.c. Systems', Proc. IEE/Vol. 120 No. 10, Oct. 73 pp 1232.

15. Busemann, F., 'HVDC Transmission : Hunting of Rectifiers with Marked Compounding', ERA report B/T, 104, 1951.

16. Bo Zhou, 'Steady State Stability Analysis of HVDC Systems with Digital Control', IEEE Trans. Vol. 102 No.6 June 83 pp. 1764-1770.

17. E. Uhlmann, 'Power Transmission by Direct Current', Springer-Verlag, Berlin, 1975.

18. J.P. Bowles, 'Multiterminal HVDC System Incorporating Diode Rectifier Station', IEEE PAS Vol. 100, No.4, April 81, pp. 1674.

19. J.L. Hay, J.S. Bhatti and N.G. Hingorani, 'Simplified Dynamic Simulation of HVDC System by Digital Computer', IEEE Trans. Vol. 19, No.2. March'71.

20. N. Sato, N.V. Dravid, S.M. Chan, A.L. Burns and J.J. Vithayathil, 'Multiterminal HVDC System Representation in a Transient Stability Program', IEEE Trans, Vol. PAS 99, pp 1927-1935, Sept/Oct. 1980.